

000 001 002 003 004 005 SCULPTOR: EMPOWERING LLMs WITH COGNITIVE 006 AGENCY VIA ACTIVE CONTEXT MANAGEMENT 007 008 009

010 **Anonymous authors**
011 Paper under double-blind review
012
013
014
015
016
017
018
019
020
021
022
023
024
025
026
027
028
029

030 ABSTRACT 031

032 Large Language Models (LLMs) suffer from significant performance degradation
033 when processing long contexts due to proactive interference, where irrelevant infor-
034 mation in earlier parts of the context disrupts reasoning and memory recall. While
035 most research focuses on external memory systems to augment LLMs’ capabilities,
036 we propose a complementary approach: empowering LLMs with Active Context
037 Management (ACM) tools to actively sculpt their internal working memory. We
038 introduce **Sculptor**, a framework that equips LLMs with three categories of tools:
039 (1) context fragmentation, (2) summary, hide, and restore, and (3) precise search.
040 Our approach enables LLMs to proactively manage their attention and working
041 memory, analogous to how humans selectively focus on relevant information while
042 filtering out distractions. Experimental evaluation on diverse long-context bench-
043 marks demonstrates that **Sculptor** significantly improves performance even without
044 specific training, leveraging LLMs’ inherent tool-calling and instruction-following
045 capabilities. To further optimize these strategies, we introduce a novel dynamic
046 context-aware reinforcement learning (RL) approach, advancing the training of
047 an agent that actively modifies its own conversational history. By enabling Ac-
048 tive Context Management, **Sculptor** not only mitigates proactive interference but
049 also provides a cognitive foundation for more reliable reasoning across diverse
050 long-context tasks—highlighting that explicit context-control strategies, rather than
051 merely larger token windows, are key to robustness at scale.
052

053 1 INTRODUCTION

054 Large Language Models (LLMs) have demonstrated remarkable capabilities across diverse tasks,
055 yet they face fundamental challenges when processing long contexts. Prior work shows that simply
056 enlarging the context window leaves models vulnerable to position bias, overload, and interference as
057 sequences grow (Liu et al., 2023a; Hsieh et al., 2024a). Recent studies (Wang & Sun, 2025) have
058 empirically demonstrated that LLMs suffer from proactive interference, where earlier information in
059 the context disrupts the processing of subsequent, more relevant information. Moreover, calibrations
060 like Found in the Middle (Hsieh et al., 2024b) reduce—but do not eliminate—positional bias; recent
061 evaluations (Tian et al., 2025) find that performance still degrades significantly when the distance
062 between relevant information pieces increases, as irrelevant information between them interferes with
063 effective information integration. These phenomena mirror human cognitive psychology, where new
064 learning can be impaired by previously acquired information that is no longer relevant to the current
065 task.

066 The challenge becomes particularly acute in complex, multi-step reasoning tasks where LLMs
067 must maintain focus on multiple critical information pieces while filtering out contextual noise (Li
068 et al., 2025a). Traditional approaches to address long-context challenges have primarily focused on
069 expanding context windows or developing external memory systems (Li et al., 2025c; Yang et al.,
070 2024; Wang & Chen, 2025; Chhikara et al., 2025; Packer et al., 2024; Wang et al., 2024; Suzgun
071 et al., 2025). While these solutions increase the amount of information an LLM can access, they do
072 not address the fundamental issue of proactive interference—**the inability to actively manage and**
073 **curate the working memory that directly influences reasoning processes.**

074 Consider a human expert working on a complex problem: they naturally employ active memory
075 management strategies, selectively attending to relevant information, summarizing key insights, and

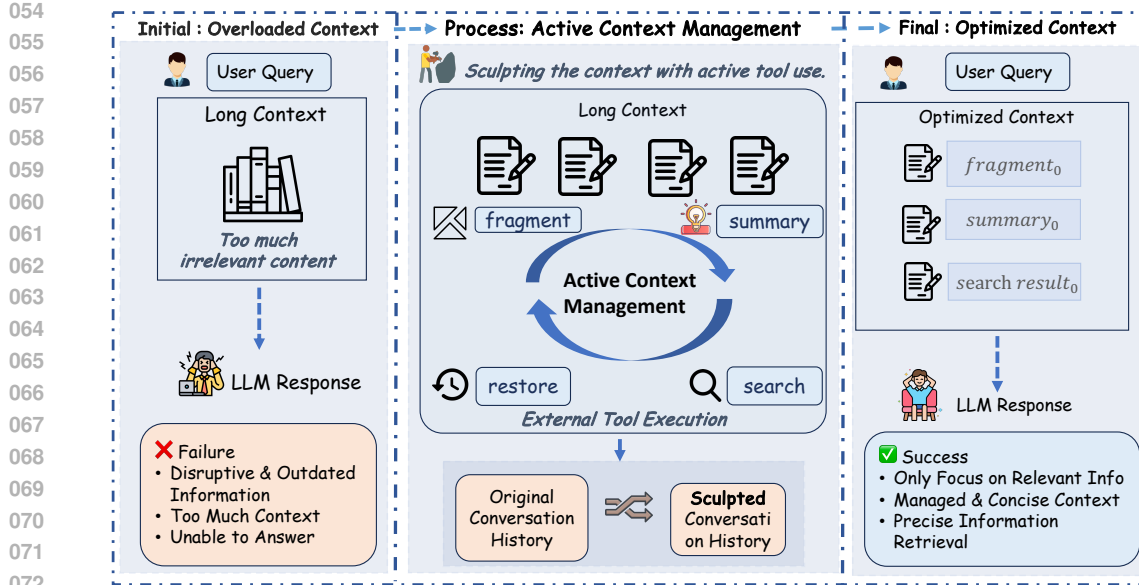


Figure 1: Overview of **Sculptor** framework: Through Active Context Management, LLMs transform overloaded contexts into optimized contexts using fragment, summary, search, and restore operations, enabling successful task completion where traditional approaches fail due to interference.

temporarily setting aside less important details. They can revisit previously discarded information when needed, but crucially, they do not allow irrelevant details to continuously interfere with their current reasoning process. Current LLMs lack this fundamental cognitive capability. We propose that the solution lies not merely in expanding context window, but in **empowering LLMs with the ability to actively manage their internal working memory**. Following established distinctions in Li et al. (2024a); Guo et al. (2024), we focus on optimizing the model’s working memory—the immediate context where attention operates and reasoning occurs—rather than external memory systems that store information outside the model’s immediate context.

To this end, we introduce **Sculptor**, a novel framework that treats LLMs as active sculptors of their own context. Just as a sculptor views a block of marble and selectively removes material to reveal the desired form, **Sculptor** achieves this through a process we call Active Context Management (ACM), as illustrated in Figure 1. We equip LLMs with the **Sculptor** tool suite that enables them to: (1) **Fragment and Organize**: Segment long conversations into manageable pieces with unique IDs for easy reference. (2) **Summary, Hide, and Restore**: Generate focused summaries, dynamically fold irrelevant sections to reduce clutter, and flexibly restore or expand content as needed. (3) **Search and Retrieve**: Perform both exact and semantic searches to quickly locate relevant information

This approach represents a paradigm shift from passively processing ever-growing contexts to active context curation. Instead of being overwhelmed by increasingly long contexts, LLMs learn to proactively manage their attention and working memory, focusing computational resources on the most relevant information. We view **Sculptor** as a representative of this emerging direction—complementary to external memory systems (Li et al., 2025c; Yang et al., 2024; Wang & Chen, 2025; Chhikara et al., 2025; Packer et al., 2024; Wang et al., 2024; Yu et al., 2025) that focus on cross-session persistence and context extension approaches—providing a necessary step toward reliable long-horizon reasoning. Related work on context compression (Xu et al., 2023; Jiang et al., 2024b; Guo et al., 2025) further demonstrates that selectively foregrounding key information can simultaneously improve accuracy and reduce cost and latency, reinforcing the need for explicit context control over passive attention alone. Recent work also suggests that in-context learning can be viewed as implicit weight updates (Dherin et al., 2025), implying that allowing models to modify their own context enables a form of “self-evolution” (Zhang et al., 2025a)—a step toward agents that can adapt their computational substrate without external intervention.

Our key contributions are as follows:

- 108 • We propose Active Context Management (ACM) for LLMs and realize it with Sculptor, a
109 toolkit that enables principled, systematic optimization of internal working memory through
110 active context manipulation.
- 111 • We propose an RL training approach for active context modification, introducing Conditional
112 Trajectory Collection and Incremental Loss Assignment to enable effective learning of
113 context manipulation strategies. Through dynamic context-aware GSPO training, we achieve
114 substantial performance gains across diverse long-context benchmarks.
- 115 • We provide comprehensive analysis of tool usage patterns, attention mechanisms, and cost
116 analysis, demonstrating that ACM effectively reduces context token consumption while
117 enhancing long-context capabilities.

119 2 METHODOLOGY

120 **Sculptor** introduces a paradigm shift in how LLMs handle their working memory. Instead of passively
121 accepting all information in their context window, we empower models to actively manage their
122 attention through a suite of context manipulation tools. Our framework operates on the principle that
123 intelligent information curation is as important as information capacity.

124 2.1 TOOL DESIGN PRINCIPLES

125 Our tool design follows four core principles. (1) **Deterministic and Self-Contained Operations**:
126 each tool is a simple, deterministic operator without external dependencies (e.g., embedding models),
127 a self-contained design that guarantees deployment stability and isolates the LLM’s cognitive agency
128 for pure evaluation. (2) **Cognitive Alignment**: the tools mirror effective human strategies, such
129 as our `search_context` tool performing exact matching akin to “Ctrl+F”, a computationally
130 efficient approach that reserves complex semantic understanding for the LLM’s own reasoning. (3)
131 **Structural Preservation for Scalable Training**: the tools are constrained to never alter the count
132 or order of messages, thereby maintaining a stable state representation that is critical for tractable
133 credit assignment in reinforcement learning. (4) **Reversibility and Graceful Degradation**: All
134 context-modifying operations are designed to be non-destructive and fully reversible (e.g., `fold` is
135 undone by `expand`), ensuring no information is permanently lost. This guarantees that the framework
136 functions as a strict superset of the baseline model’s capabilities, allowing for graceful degradation:
137 if no tools are invoked, the model’s behavior is identical to its original, unmodified state.

138 2.2 THE SCULPTOR TOOL SUITE

139 Following these design principles, we equip LLMs with six fundamental tools organized into three
140 functional categories, allowing them to work in coordination within a single turn, where the agent
141 receives a user message and performs multi-step tool calls—for instance, fragmenting a context
142 segment yields a unique fragment ID that enables subsequent operations like compression, summa-
143 rization, or restoration—continuously invoking these tools until generating a final response without
144 further tool invocations. Complete JSON schemas for all tools are provided in Appendix H.

145 (1) *Context Fragmentation* is handled by `fragment_context`, which segments long conversations
146 into manageable fragments using start and end markers, with each fragment receiving a unique 6-
147 character ID for easy reference.

148 (2) *Context Compression and Restoration* involves three complementary tools for dynamic con-
149 tent management. `summarize_fragment` generates focused AI-powered summaries of specific
150 fragments based on user-specified focus areas (e.g., technical details, key decisions, action items),
151 compressing content while preserving critical information. `fold_fragment` temporarily hides
152 fragment content while preserving its existence, displaying only a folded marker to dramatically
153 reduce visual clutter. `restore_fragment` provides universal restoration capability, reverting
154 both summarized and folded fragments back to their original content, ensuring no information is
155 permanently lost during context management operations.

156 (3) *Precise Search and Retrieval* is accomplished through two complementary tools.
157 `search_context` performs exact keyword matching across user messages, assistant responses, or
158 all content—mirroring the human approach of using Ctrl+F for information retrieval. It returns up to

162 50 matches with configurable result context windows. `get_search_detail` retrieves extended
 163 context around specific search results, with the model specifying the desired surrounding character
 164 count. By appending search results to the end of conversation history, this approach mitigates the
 165 “lost in the middle” problem (Liu et al., 2023a) where models struggle to locate information buried
 166 within long contexts.
 167

168 3 TEACHING LLMs TO USE SCULPTOR TOOLS

170 Building on the strong tool-use capabilities inherent in modern LLMs, we explore two distinct
 171 approaches for teaching models to effectively wield the **Sculptor** tool suite. Throughout this paper,
 172 we use “ACM tools” to specifically refer to our **Sculptor** implementation—a concrete instantiation of
 173 the broader Active Context Management paradigm.
 174

175 3.1 INHERENT TOOL-USE PERFORMANCE

177 We first evaluate the inherent tool-calling capabilities of state-of-the-art models like Claude-4-Sonnet
 178 and GPT-4.1, which demonstrate strong zero-shot generalization abilities for function calling. These
 179 models can understand and execute our **Sculptor** tools without any specific training, relying on
 180 their pre-trained understanding of tool usage patterns and natural language descriptions of tool
 181 schema. This zero-shot approach requires no additional training—models directly interpret and
 182 use the tools based solely on their schemas. To encourage consistent tool engagement, we set
 183 `tool_choice`=“required” for the first step of multi-step conversations.
 184

185 3.2 MULTI-STEP AGENT RL TRAINING WITH DYNAMIC CONTEXT-AWARE GSPO

186 To optimize tool usage strategies beyond zero-shot generalization, we develop a reinforcement
 187 learning approach specifically designed for multi-step tool calling in long-context scenarios. Our
 188 approach addresses the unique challenges of training models to actively manage dynamic contexts
 189 where tool calls can fundamentally alter the information landscape.
 190

191 **Group Sequence Policy Optimization (GSPO).** We adapt GSPO (Zheng et al., 2025) for multi-
 192 step rl training, leveraging its sequence-level optimization for stable training in long-context scenarios.
 193 Given a query x and G sampled trajectories $\{\tau_i\}_{i=1}^G$ from policy $\pi_{\theta_{\text{old}}}$, GSPO optimizes:

$$195 \mathcal{J}_{\text{GSPO}}(\theta) = \mathbb{E}_{x \sim \mathcal{D}} \left[\frac{1}{G} \sum_{i=1}^G \min \left(s_i(\theta) \hat{A}_i, \text{clip}(s_i(\theta), 1 - \varepsilon, 1 + \varepsilon) \hat{A}_i \right) \right] \quad (1)$$

196 where the sequence-level importance ratio is:
 197

$$199 s_i(\theta) = \left(\frac{\pi_\theta(\tau_i|x)}{\pi_{\theta_{\text{old}}}(\tau_i|x)} \right)^{\frac{1}{|\tau_i|}} \quad (2)$$

200 and the group-normalized advantage is:
 201

$$204 \hat{A}_i = \frac{r(x, \tau_i) - \text{mean}(\{r(x, \tau_j)\}_{j=1}^G)}{\text{std}(\{r(x, \tau_j)\}_{j=1}^G)} \quad (3)$$

205 **Dynamic Context-Aware Credit Assignment with Incremental Loss Design.** The key innovation
 206 in our approach addresses the non-monotonic nature of context evolution during tool calling.
 207 Traditional multi-step RL assumes each trajectory τ_t is a prefix of τ_{t+1} , allowing training only
 208 on the final trajectory. However, with context management tools, $c_t \not\subset c_{t+1}$ in general—tools like
 209 `fold_fragment` or `summarize_fragment` actively remove or transform information, creating
 210 divergent context states.
 211

212 To handle this, we introduce a two-part strategy combining **conditional trajectory collection** and
 213 **incremental loss assignment**, illustrated in Figure 2 and detailed in Appendix E. The final reward
 214 is propagated to all sub-trajectories within the same rollout, ensuring each context state receives
 215 appropriate learning signal. This incremental design prevents the model from learning spurious

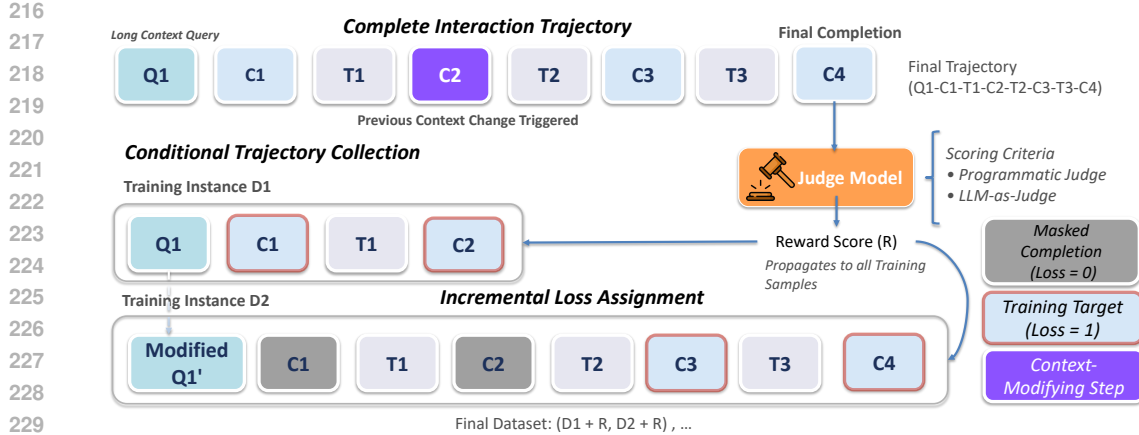


Figure 2: Conditional trajectory collection and incremental loss assignment for RL training. Q represents the initial user context, C denotes assistant completions, and T indicates tool results. Top: Complete interaction trajectory with context-modifying tool at step C2. Bottom: Training samples extracted via conditional trajectory collection, where each context change creates a new training instance. Incremental loss is assigned only to new completions (red boxes) while masking prior completions (loss=0), preventing redundant learning and training collapse.

patterns where context-modifying tools repeatedly trigger themselves, which would cause training collapse. Each tool call receives gradient signal exactly once across all completions, ensuring stable and efficient learning. Notably, this method applies equally to both supervised fine-tuning (SFT) and reinforcement learning stages, providing a unified framework for training with dynamic contexts.

4 EXPERIMENTS

We evaluate **Sculptor** in two settings: zero-shot tool calling leveraging models' inherent capabilities, and after reinforcement learning with dynamic context-aware GSPO to optimize tool usage strategies.

4.1 EVALUATING PROMPT-GUIDED TOOL CALLING PERFORMANCE

Evaluated Models: We evaluate the effectiveness of **Sculptor** by comparing LLMs with and without the **Sculptor** tool suite across challenging benchmarks. Our experiments focus on Claude-4-Sonnet (Anthropic, 2025), GPT-4.1 (OpenAI, 2025), and DeepSeek-V3 (DeepSeek-AI et al., 2024) as representative state-of-the-art models, testing both baseline configurations and **Sculptor**-enhanced versions.

Evaluated Benchmarks: We evaluate on five benchmarks testing diverse long-context challenges: (1) **PI-LLM** (Wang & Sun, 2025) tests proactive interference through continuous key-value updates (2-256 updates, 46 keys). (2) **NeedleBench** (Li et al., 2025a) Multi-Needle Reasoning requires connecting 2-5 needles simultaneously across varying context lengths. For cost efficiency and rapid validation, we initially evaluate only on PI-LLM and NeedleBench in zero-shot settings. After RL training, we expand to: (3) **MRCR** (Vodrahalli et al., 2024a) for multi-round co-reference resolution, requiring models to distinguish between multiple identical requests (2-8 needles) and return the i-th occurrence from synthetic conversations. (4) **LongBenchV2** (Bai et al., 2025) for comprehensive long-context understanding. (5) **FRAMES** (Krishna et al., 2025) for factuality, retrieval, and reasoning measurement, containing 824 multi-hop questions requiring integration of information from 2-15 Wikipedia articles.

Inherent Challenges of Unguided Tool Use: To understand how models naturally interact with ACM tools, we conducted initial experiments using Claude-4-Sonnet on PI-LLM and NeedleBench benchmarks, collecting 50 samples from each benchmark for tool usage analysis. We provided

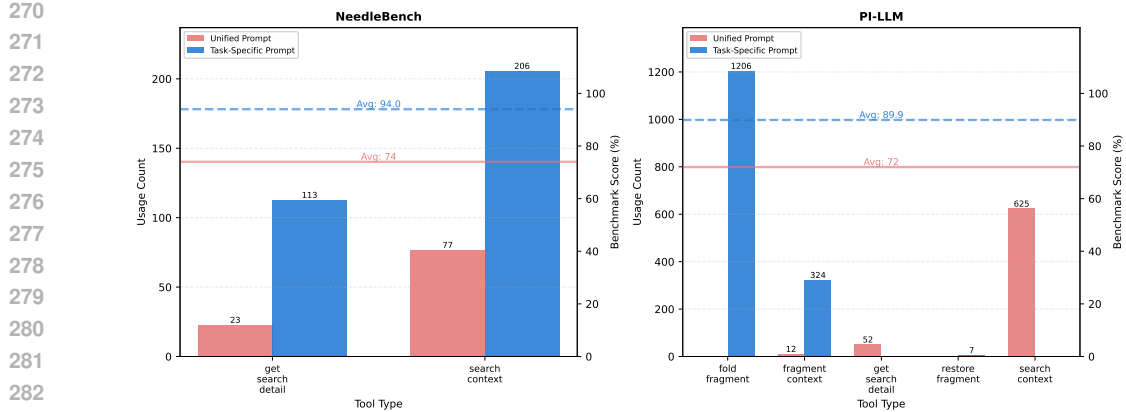


Figure 3: Tool usage count comparison for Claude-4-Sonnet before and after prompt optimization. Without task-specific prompts (unified prompt), both benchmarks show suboptimal patterns. With benchmark-specific prompt engineering, distinct improvements emerge: PI-LLM shifts from inefficient search-heavy patterns (625 calls) to strategic `fold_fragment` usage (1206 calls) for managing obsolete information, while NeedleBench increases search operations from 77 to 206 calls—addressing insufficient execution depth through more thorough verification and multi-hop reasoning. These contrasting patterns highlight how prompt engineering resolves different challenges: tool selection efficiency for PI-LLM versus execution completeness for NeedleBench.

the model with a unified system prompt—minimal, generic instructions applicable across all tasks—without any benchmark-specific guidance (see Appendix D.2 for the complete prompt).

Our findings revealed suboptimal tool selection patterns, as shown in Figure 3 (left bars). For PI-LLM, which contains numerous obsolete key-value pairs requiring the model to focus on the latest mappings, we expected the model to leverage `fragment_context` and `fold_fragment` to compress outdated information. However, Claude-4-Sonnet overwhelmingly relied on `search_context` (90.7% of tool calls), attempting exhaustive searches for each of the 46 keys despite hundreds of historical updates per key. This search-heavy approach proved highly inefficient—the model exhausted its 20-tool-call budget merely aggregating occurrences without effectively filtering obsolete information. Similarly, for NeedleBench, while search tools are appropriate for retrieval tasks, the model showed limited strategic diversity in tool selection.

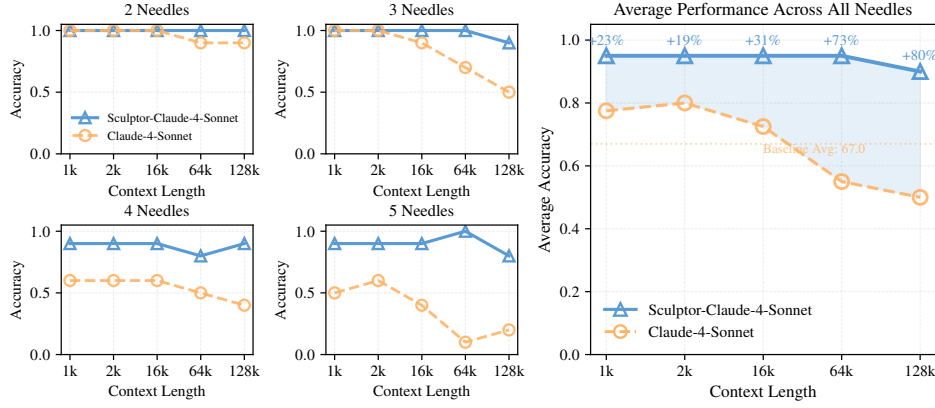
These observations reveal three fundamental challenges in unguided tool calling: (1) **Suboptimal tool selection efficiency**: The model failed to recognize when certain tools become inefficient for specific scenarios. In PI-LLM, attempting exhaustive searching for 46 keys with hundreds of historical updates each consumed the entire tool budget, when structural reorganization through fragment-and-fold would have been far more efficient. (2) **Tool dependency misunderstanding**: The model lacked comprehension of tool prerequisites and operational dependencies—for instance, attempting to use `summary_by_id` before generating fragment IDs with `fragment_context`, demonstrating incomplete understanding of the tool suite’s workflow. (3) **Insufficient execution depth**: Even when correctly initiating tool usage, the model often failed to complete tasks thoroughly, with incomplete fragmentation where only partial sections were processed, leaving critical information unaddressed. These challenges underscore that effective ACM tool usage requires not just access to tools but deep understanding of efficiency trade-offs, operational dependencies, and thorough execution strategies.

From Baseline Struggles to Systematic Guidance: To address these inefficiencies, we crafted benchmark-specific prompts to steer tool strategies: for PI-LLM, first `fragment` then `fold` before any search or answering; for NeedleBench, coordinate `search_context` and `get_search_detail` for multi-hop retrieval. As shown in Figure 3, this guidance shifts patterns accordingly (PI-LLM: from search-heavy to fragment+fold; NeedleBench: deeper search), improving tool selection efficiency and execution completeness.

This systematic prompt engineering approach also enabled us to generate high-quality training data, collecting numerous successful tool usage examples across benchmarks. These guided patterns

324 Table 1: Performance improvements of frontier models with ACM Tools on NeedleBench-M-RS and
 325 PI-LLM benchmarks. Both benchmarks demonstrate substantial performance gains.
 326

327 Method	328 NeedleBench-M-RS					329 PI-LLM (Update Count / Context Length)							
	330 2-N	3-N	4-N	5-N	Avg	331 4/1K	8/2K	16/4K	32/8K	64/16K	128/32K	256/64K	Avg
Claude-4-Sonnet													
Baseline	96.0	82.0	54.0	36.0	67.0	99.13	95.65	92.17	84.78	81.74	65.22	69.57	84.04
w/ ACM Tools	100.0	98.0	88.0	90.0	94.0	90.43	91.74	98.26	92.17	91.74	87.39	77.83	89.94
Δ	+4.0	+16.0	+34.0	+54.0	+27.0	-8.70	-3.91	+6.09	+7.39	+10.00	+22.17	+8.26	+5.90
GPT-4.1													
Baseline	90.0	64.0	30.0	8.0	48.0	96.96	91.30	79.57	67.83	63.04	63.91	50.43	73.29
w/ ACM Tools	96.0	84.0	60.0	44.0	71.0	92.17	89.13	93.04	83.91	76.09	64.35	60.43	79.87
Δ	+6.0	+20.0	+30.0	+36.0	+23.0	-4.79	-2.17	+13.47	+16.08	+13.05	+0.44	+10.00	+6.58
DeepSeek-V3													
Baseline	88.0	68.0	28.0	16.0	50.0	95.22	85.65	70.00	63.91	33.04	32.17	21.74	57.39
w/ ACM Tools	92.0	58.0	50.0	32.0	58.0	73.91	90.00	79.13	37.39	53.04	55.65	11.74	57.27
Δ	+4.0	-10.0	+22.0	+16.0	+8.0	-21.31	+4.35	+9.13	-26.52	+20.00	+23.48	-10.00	-0.12



353 Figure 4: NeedleBench Multi-Needle Reasoning performance across different context lengths. Left:
 354 Performance by needle count showing both with tool and vanilla results. Right: Average performance
 355 across all needle counts demonstrating significant improvements.
 356

358 demonstrate that proper instruction can unlock more effective tool utilization, transforming suboptimal
 359 default behaviors into strategic, task-appropriate tool selection. The complete system prompt
 360 templates used in our experiments are provided in Appendix D.1.
 361

362 **Performance Results:** Table 1 presents the evaluation results comparing models with and without
 363 ACM tools, using optimized benchmark-specific prompts. The improvements demonstrate the power
 364 of combining ACM tools with proper guidance: On NeedleBench-M-RS, Claude-4-Sonnet, GPT-4.1,
 365 and DeepSeek-V3 achieve gains of 27.0, 23.0, and 8.0 points respectively when using ACM tools
 366 with task-specific prompts, with Claude-4-Sonnet reaching 90% accuracy on 5-needle tasks. For
 367 PI-LLM, Claude-4-Sonnet and GPT-4.1 gain 5.90 and 6.58 points, while DeepSeek-V3 shows a
 368 slight decrease (-0.12), revealing persistent challenges even with prompt optimization. These results
 369 demonstrate that while prompt engineering significantly improves tool utilization, the degree of
 370 improvement varies based on each model’s inherent tool-use capabilities, suggesting the need for
 371 more systematic training approaches.
 372

373 4.2 OPTIMIZING TOOL USE WITH REINFORCEMENT LEARNING

375 While prompt engineering enables effective tool usage, it requires manual effort to design task-specific
 376 prompts and still exhibits the inherent limitations discussed above. To address these challenges
 377 systematically, we employ reinforcement learning to train models that can autonomously determine
 378 optimal tool usage strategies without explicit guidance.
 379

378 Table 2: Main experimental results across benchmarks. M3 indicates our 13B baseline model without
 379 ACM tools. Sculptor-M3 is equipped with **Sculptor** tools and fine-tuned on ACM-specific data.
 380 Sculptor-M3-RL is further trained with dynamic context-aware GSPO. Similar notation applies to
 381 GLM-4.5-air models. **Bold** indicates best performance, underline indicates second best.

Method	PI-LLM (Acc %)	NeedleBench-M-RS (Acc %)	MRCR (Acc %)	LongBenchV2 (Acc %)	Frames (Acc %)	Avg (Norm)
M3 (Baseline)	22.5	30.0	46.3	<u>33.0</u>	65.2	39.4
M3 + RAG (BM25)	17.9	12.5	6.6	25.8	33.6	19.3
M3 + RAG (Qwen3-Emb)	10.9	13.0	20.6	29.6	46.0	24.0
M3 + Mem0	39.2	19.0	9.2	29.0	52.8	29.8
M3 + MemAgent	41.5	24.0	22.1	29.6	61.5	35.7
Sculptor-M3	<u>71.8</u>	<u>67.6</u>	<u>79.1</u>	29.2	51.2	<u>59.8</u>
Sculptor-M3-RL	99.4	84.8	85.7	34.5	<u>64.6</u>	73.8
GLM-4.5-air(Baseline)	29.4	24.5	43.1	<u>46.9</u>	<u>76.0</u>	44.0
GLM-4.5-air + RAG (BM25)	30.6	15.0	4.8	19.5	30.9	20.2
GLM-4.5-air + RAG (Qwen3-Emb)	10.9	12.0	24.1	27.2	46.6	24.2
GLM-4.5-air + Mem0	18.5	14.5	6.2	28.8	62.3	26.1
GLM-4.5-air + MemAgent	22.2	17.0	8.6	33.2	68.6	29.9
Sculptor-GLM-4.5-air	<u>65.2</u>	<u>58.0</u>	<u>88.5</u>	31.7	56.7	<u>60.0</u>
Sculptor-GLM-4.5-air-RL	86.0	84.0	99.0	50.7	79.2	79.8

397 **Model and baselines.** We base our experiments on both an internal model and an open-source
 398 model to demonstrate the effectiveness and generalizability of our approach. Our primary model
 399 is M3, a 13B-parameter dense model that we pre-train from scratch, chosen for its strong tool-use
 400 capabilities (see Appendix C), tight compatibility with our training infrastructure, and competitive
 401 baseline performance. To validate the generalizability of our approach beyond proprietary models, we
 402 additionally evaluate GLM-4.5-air (Team et al., 2025a), an open-source MoE model with 106B total
 403 parameters and 12B active parameters. In Table 2, we additionally compare three baseline approaches
 404 (all implemented on the same M3 base model for controlled comparison): retrieval-augmented
 405 generation (RAG), Mem0 (Chhikara et al., 2025) representing cross-session external memory, and
 406 MemAgent (Yu et al., 2025) as an inner working memory method. We evaluate RAG with both BM25
 407 (keyword matching) and Qwen3-Emb (dense retrieval), representing both traditional and modern
 408 RAG approaches. Further evaluation details are provided in Appendix D.4.

409 **Training Data Collection.** While M3 possesses strong inherent tool-use capabilities, it requires
 410 specific training to effectively utilize the **Sculptor** tools. We generate high-quality training data
 411 through the systematic prompt engineering approach described in Section 4.1. Using Claude-4-
 412 Sonnet with carefully designed task-specific prompts, we collect successful tool usage trajectories
 413 on the BABILong (Kuratov et al., 2024) and GSM-Infinite (Zhou et al., 2025) datasets—public
 414 benchmarks featuring complex long-context reasoning challenges. This process yields diverse
 415 examples of effective ACM tool usage patterns across different task types. Combined with our
 416 conditional trajectory collection and incremental loss assignment methodology (Section 3.2), we first
 417 perform supervised fine-tuning on this data to obtain Sculptor-M3, which has learned basic ACM tool
 418 capabilities. Subsequently, we conduct RL training with dynamic context-aware GSPO on the same
 419 datasets to obtain Sculptor-M3-RL, enabling the model to autonomously discover optimal tool usage
 420 strategies. During training, we cap tool steps at 20 per turn, matching Claude-4-Sonnet’s effective
 421 zero-shot usage while keeping rollouts efficient.

422 **Experimental Results:** Table 2 presents our experimental results. Sculptor-M3 shows improve-
 423 ments over baseline M3, particularly on PI-LLM (+49.3 points), NeedleBench-M-RS (+37.6 points),
 424 and MRCR (+32.8 points). After GSPO training on BABILong and GSM-Infinite datasets, Sculptor-
 425 M3-RL reaches 99.4% on PI-LLM with gains across most benchmarks. Additionally, we evaluate
 426 GLM-4.5-air, an open-source model, demonstrating that our approach generalizes beyond our prop-
 427 erty base model. GLM-4.5-air with **Sculptor** achieves substantial improvements over its baseline
 428 (+35.8 on PI-LLM, +33.5 on NeedleBench-M-RS, +45.4 on MRCR), reaching 60.0% average per-
 429 formance and confirming the effectiveness of our ACM tools across different model architectures.
 430 Detailed analysis of RL training dynamics and tool usage evolution is provided in Appendix G.

431 A critical observation from Table 2 is that **only our Sculptor approach with RL training surpasses**
 432 **or achieves comparable performance to the full-attention baseline** for both M3 and GLM-4.5-air.

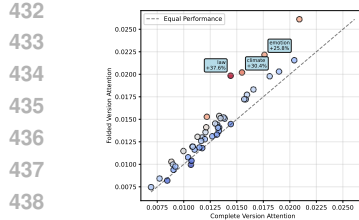


Figure 5: Value-specific attention analysis results. Left: Scatter plot comparing attention weights between folded and complete versions for 46 key-value pairs. Most points lie above the equality line, indicating improved attention with folding. Right: Distribution of attention improvements, showing a clear positive shift and confirming the systematic benefit of our approach.

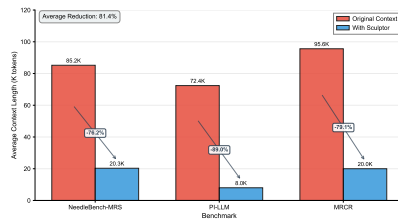


Figure 6: Average context length reduction with Sculptor across benchmarks. Arrows indicate reduction percentages achieved through strategic tool usage.

Traditional methods all fall short of their respective baselines: RAG methods introduce information loss through irreversible retrieval, achieving only 19.3% (BM25) and 24.0% (Qwen3-Emb) average for M3, and 20.2% (BM25) and 24.2% (Qwen3-Emb) for GLM-4.5-air. MemAgent’s query-dependent memory accumulation discards information that appears initially irrelevant but proves critical for multi-hop reasoning—achieving 35.7% average for M3 and 29.9% for GLM-4.5-air, both below their respective baselines (39.4% and 44.0%). Mem0 underperforms MemAgent across most benchmarks, likely because it is designed for cross-session personalized memory rather than single-session long-context scenarios. The fundamental limitation is that these methods make irreversible filtering decisions based solely on the final query, without the ability to recover information that becomes relevant only after seeing subsequent context. In contrast, our ACM tools enable reversible context management—folding currently irrelevant information while preserving restoration capability. This flexibility allows Sculptor-M3-RL to reach 73.8% average (vs. 39.4% baseline) and **Sculptor**-GLM-4.5-air-RL to reach 79.8% average (vs. 44.0% baseline), demonstrating that our approach fundamentally addresses the limitations of prior methods by maintaining information accessibility rather than discarding it.

4.3 VALUE-SPECIFIC ATTENTION ANALYSIS

To precisely quantify how content folding impacts attention allocation to critical information, we conduct a token-level value-specific attention analysis. While traditional approaches assume that attention mechanisms naturally learn to ignore irrelevant information during pretraining, our analysis reveals that explicitly removing distracting content significantly enhances attention focus. The core idea is to measure the attention from the tokens of a specific critical value in the model’s response back to the corresponding tokens of the same value in the input context. Our experiment uses 46 predefined key-value pairs from the PI-LLM benchmark as the critical information. For each pair, we calculate the attention score by first identifying the exact token positions of the value in both the input and the response. We then aggregate the attention weights across all layers and heads, averaging them to produce a single score that represents the model’s focus on that specific piece of information. This allows for a direct comparison between the “folded” context and the “complete” context scenarios. The results presented in Figure 5 demonstrate a significant and systematic improvement in attention allocation. Out of 46 key-value pairs, 43 (93.5%) exhibited enhanced attention in the folded version, achieving a mean improvement of 9.87% (ranging from -6.86% to +37.56%). The scatter plot reveals a strong positive correlation ($R^2 = 0.97$) with the vast majority of data points positioned above the equality line, confirming that the improvements are consistent and not random.

Notable performance gains were observed for pairs such as “law: contract” (+37.56%), “climate: heat dome” (+30.44%), and “emotion: indifferent” (+25.83%). A one-sample t-test on the distribution of improvements confirms that they are statistically significant ($p < 0.001$), with a median improvement of 9.9%. These findings provide strong empirical evidence that folding redundant content enhances attention allocation to critical information by reducing attention dilution—even in well-pretrained models, irrelevant information interferes with attention mechanisms rather than being naturally filtered

486 out. The consistent improvements across diverse semantic categories suggest that explicit context
 487 management through folding is more effective than relying solely on learned attention patterns.
 488

489 **4.4 COST ANALYSIS**
 490

491 To evaluate the computational efficiency of our approach, we analyze the context reduction achieved
 492 by Sculptor-M3-RL on benchmarks containing substantial irrelevant information. As shown in
 493 Figure 6, Sculptor-M3-RL achieves dramatic context reductions across these challenging benchmarks:
 494 76.2% reduction on NeedleBench-M-RS (from 85.2K to 20.3K tokens), 89.0% on PI-LLM (from
 495 72.4K to 8.0K tokens), and 79.1% on MRCR (from 95.6K to 20.0K tokens). These substantial
 496 reductions directly translate to computational savings, as the quadratic complexity of attention
 497 mechanisms makes processing cost heavily dependent on context length.
 498

499 Importantly, our tool design minimizes additional computational overhead. Read-only tools like
 500 `search_context` preserve the prefix relationship between completions and fully reuse KV
 501 cache—they only add a few search operations while most of the context remains cached. This
 502 is similar to traditional tool use where KV cache can be efficiently reused. For context-modifying
 503 tools that do break the prefix relationship, the dramatic context reduction itself compensates for the
 504 cache invalidation cost. Processing 20K tokens even without caching is significantly faster than
 505 processing 85K tokens with full caching. This design—separating context-preserving search tools
 506 from context-modifying compression tools—ensures that our system achieves substantial context
 507 reduction with minimal computational overhead.
 508

509 **5 LIMITATIONS AND FUTURE WORK**
 510

511 Our study primarily targets long-context scenarios, but ACM is also promising beyond long contexts.
 512 In mathematical reasoning, early mistakes can cascade due to autoregressive “prefix lock-in” that
 513 degrades subsequent correctness; folding or suppressing erroneous early steps may reset the trajectory
 514 and improve robustness (Wang & Sun, 2025; Feng et al., 2025; Wen et al., 2025). Future work will
 515 extend ACM to non-long-context domains (e.g., math, coding) and pursue richer training strategies
 516 and reward design to learn finer-grained tool-use policies, with the goal of improving performance on
 517 complex long-context benchmarks where our current results remain modest, such as LongBenchV2
 518 and FRAMES (Bai et al., 2025; Krishna et al., 2025).
 519

520 **ETHICS STATEMENT**
 521

522 This work focuses on improving the efficiency and effectiveness of large language models in handling
 523 long contexts through active context management. Our research does not involve human subjects,
 524 and all experiments were conducted on publicly available benchmarks. We acknowledge that context
 525 manipulation tools could potentially be misused to selectively remove or hide information in harmful
 526 ways. However, our work is designed to enhance model performance on legitimate tasks by helping
 527 models focus on relevant information while maintaining the ability to restore folded content when
 528 needed. We are committed to responsible AI development and encourage the community to consider
 529 both the benefits and potential risks of active context management techniques when deploying such
 530 systems.
 531

532 **REPRODUCIBILITY STATEMENT**
 533

534 To ensure reproducibility of our results, we provide comprehensive details throughout the paper and
 535 supplementary materials. Our ACM tool implementations are described in detail in Appendix H,
 536 with complete schemas. The GSPO training methodology is fully specified in Section 2, with
 537 hyperparameters and hardware configurations detailed in Table 4. The dynamic context-aware
 538 training data collection algorithm is provided in Algorithm 1. All experiments were conducted on
 539 publicly available benchmarks (PI-LLM, NeedleBench, MRCR, LongBenchV2, and Frames) with
 540 configurations detailed in Appendix D. We will release our code for Algorithm 1, **Sculptor** tools
 541 implementations and trained model checkpoints upon acceptance to facilitate reproduction and further
 542 research.
 543

540 REFERENCES
541

542 Anthropic. System Card: Claude Opus 4 & Claude Sonnet 4. <https://www-cdn.anthropic.com/4263b940cabb546aa0e3283f35b686f4f3b2ff47.pdf>, May 2025. Accessed: 543 2025-08-05.

544 Jacob Austin, Daniel D. Johnson, Jonathan Ho, Daniel Tarlow, and Rianne van den Berg. Structured 545 denoising diffusion models in discrete state-spaces. In *Advances in Neural Information Processing 546 Systems*, 2021.

547 Yushi Bai, Shangqing Tu, Jiajie Zhang, Hao Peng, Xiaozhi Wang, Xin Lv, Shulin Cao, Jiazheng Xu, 548 Lei Hou, Yuxiao Dong, Jie Tang, and Juanzi Li. Longbench v2: Towards deeper understanding 549 and reasoning on realistic long-context multitasks, 2025. URL <https://arxiv.org/abs/2412.15204>.

550 Victor Barres, Honghua Dong, Soham Ray, Xujie Si, and Karthik Narasimhan. τ^2 -bench: Evaluating 551 conversational agents in a dual-control environment, 2025. URL <https://arxiv.org/abs/2506.07982>.

552 Iz Beltagy, Matthew E. Peters, and Arman Cohan. Longformer: The long-document transformer, 553 2020. URL <https://arxiv.org/abs/2004.05150>.

554 Chen Chen, Xinlong Hao, Weiwen Liu, Xu Huang, Xingshan Zeng, Shuai Yu, Dexun Li, Shuai 555 Wang, Weinan Gan, Yuefeng Huang, Wulong Liu, Xinzhi Wang, Defu Lian, Baoqun Yin, Yasheng 556 Wang, and Wu Liu. Acebench: Who wins the match point in tool usage?, 2025. URL <https://arxiv.org/abs/2501.12851>.

557 Shouyuan Chen, Sherman Wong, Liangjian Chen, and Yuandong Tian. Extending context window of 558 large language models via positional interpolation, 2023. URL <https://arxiv.org/abs/2306.15595>.

559 Prateek Chhikara, Dev Khant, Saket Aryan, Taranjeet Singh, and Deshraj Yadav. Mem0: Building 560 production-ready ai agents with scalable long-term memory. *arXiv preprint arXiv:2504.19413*, 561 2025.

562 DeepSeek-AI, Aixin Liu, Bei Feng, Bing Xue, Bingxuan Wang, Bochao Wu, et al. DeepSeek-V3 563 Technical Report. <https://arxiv.org/abs/2412.19437>, December 2024.

564 Benoit Dherin, Michael Munn, Hanna Mazzawi, Michael Wunder, and Javier Gonzalvo. Learning 565 without training: The implicit dynamics of in-context learning, 2025. URL <https://arxiv.org/abs/2507.16003>.

566 Yunzhen Feng, Julia Kempe, Cheng Zhang, Parag Jain, and Anthony Hartshorn. What characterizes 567 effective reasoning? revisiting length, review, and structure of cot. 2025. doi: 10.48550/arXiv. 568 2509.19284.

569 Yizhao Gao, Zhichen Zeng, Dayou Du, Shijie Cao, Peiyuan Zhou, Jiaxing Qi, Junjie Lai, Hayden 570 Kwok-Hay So, Ting Cao, Fan Yang, and Mao Yang. Seerattention: Learning intrinsic sparse 571 attention in your llms, 2025. URL <https://arxiv.org/abs/2410.13276>.

572 Marjan Ghazvininejad, Omer Levy, Yinhan Liu, and Luke Zettlemoyer. Mask-predict: Parallel 573 decoding of conditional masked language models. In *Proceedings of the 2019 Conference on 574 Empirical Methods in Natural Language Processing and the 9th International Joint Conference on 575 Natural Language Processing (EMNLP-IJCNLP)*, pp. 6112–6121, Hong Kong, China, November 576 2019. Association for Computational Linguistics. doi: 10.18653/v1/D19-1633. URL <https://aclanthology.org/D19-1633/>.

577 Jiatao Gu, Changhan Wang, and Junbo Jake Zhao. Levenshtein transformer. In *Advances in Neural 578 Information Processing Systems*, volume 32, 2019.

579 Jing Guo, Nan Li, Jianchuan Qi, Hang Yang, Ruiqiao Li, Yuzhen Feng, Si Zhang, and Ming 580 Xu. Empowering working memory for large language model agents, 2024. URL <https://arxiv.org/abs/2312.17259>.

594 Yiju Guo, Wenkai Yang, Zexu Sun, Ning Ding, Zhiyuan Liu, and Yankai Lin. Learning to focus:
 595 Causal attention distillation via gradient-guided token pruning, 2025. URL <https://arxiv.org/abs/2506.07851>.
 596

597 Coleman Hooper, Sehoon Kim, Hiva Mohammadzadeh, Michael W. Mahoney, Yakun Sophia Shao,
 598 Kurt Keutzer, and Amir Gholami. Kvquant: Towards 10 million context length llm inference with
 599 kv cache quantization, 2025. URL <https://arxiv.org/abs/2401.18079>.
 600

601 Cheng-Ping Hsieh, Simeng Sun, Samuel Kriman, Shantanu Acharya, Dima Rekesh, Fei Jia, Yang
 602 Zhang, and Boris Ginsburg. Ruler: What's the real context size of your long-context language
 603 models?, 2024a. URL <https://arxiv.org/abs/2404.06654>.
 604

605 Cheng-Yu Hsieh, Yung-Sung Chuang, Chun-Liang Li, Zifeng Wang, Long T. Le, Abhishek Kumar,
 606 James Glass, Alexander Ratner, Chen-Yu Lee, Ranjay Krishna, and Tomas Pfister. Found in
 607 the middle: Calibrating positional attention bias improves long context utilization, 2024b. URL
 608 <https://arxiv.org/abs/2406.16008>.
 609

610 Huiqiang Jiang, Qianhui Wu, Chin-Yew Lin, Yuqing Yang, and Lili Qiu. Llmlingua: Compressing
 611 prompts for accelerated inference of large language models, 2023. URL <https://arxiv.org/abs/2310.05736>.
 612

613 Huiqiang Jiang, Qianhui Wu, Xufang Luo, Dongsheng Li, Chin-Yew Lin, Yuqing Yang, and Lili Qiu.
 614 Longllmlingua: Accelerating and enhancing llms in long context scenarios via prompt compression,
 615 2024a. URL <https://arxiv.org/abs/2310.06839>.
 616

617 Huiqiang Jiang, Qianhui Wu, Xufang Luo, Dongsheng Li, Chin-Yew Lin, Yuqing Yang, and Lili Qiu.
 618 Longllmlingua: Accelerating and enhancing llms in long context scenarios via prompt compression,
 619 2024b. URL <https://arxiv.org/abs/2310.06839>.
 620

621 Greg Kamradt. LLMs Need Needle In A Haystack Test-Pressure Testing LLMs. https://github.com/gkamradt/LLMTest_NeedleInAHaystack, 2023.
 622

623 Satyapriya Krishna, Kalpesh Krishna, Anhad Mohananey, Steven Schwarcz, Adam Stambler, Shyam
 624 Upadhyay, and Manaal Faruqui. Fact, fetch, and reason: A unified evaluation of retrieval-
 625 augmented generation, 2025. URL <https://arxiv.org/abs/2409.12941>.
 626

627 Yuri Kuratov, Aydar Bulatov, Petr Anokhin, Ivan Rodkin, Dmitry Sorokin, Artyom Sorokin, and
 628 Mikhail Burtsev. Babilong: Testing the limits of llms with long context reasoning-in-a-haystack,
 629 2024. URL <https://arxiv.org/abs/2406.10149>.
 630

631 Mo Li, Songyang Zhang, Taolin Zhang, Haodong Duan, Yunxin Liu, and Kai Chen. Needlebench:
 632 Can llms do retrieval and reasoning in information-dense context?, 2025a. URL <https://arxiv.org/abs/2407.11963>.
 633

634 Xiang Lisa Li, John Thickstun, Ishaan Gulrajani, Percy Liang, and Tatsunori B. Hashimoto. Diffusion-
 635 lm improves controllable text generation. 2022. doi: 10.48550/arXiv.2205.14217.
 636

637 Yuanchun Li, Hao Wen, Weijun Wang, Xiangyu Li, Yizhen Yuan, Guohong Liu, Jiacheng Liu,
 638 Wenxing Xu, Xiang Wang, Yi Sun, Rui Kong, Yile Wang, Hanfei Geng, Jian Luan, Xuefeng Jin,
 639 Zilong Ye, Guanjing Xiong, Fan Zhang, Xiang Li, Mengwei Xu, Zhijun Li, Peng Li, Yang Liu,
 640 Ya-Qin Zhang, and Yunxin Liu. Personal llm agents: Insights and survey about the capability,
 641 efficiency and security, 2024a. URL <https://arxiv.org/abs/2401.05459>.
 642

643 Yucheng Li, Bo Dong, Chenghua Lin, and Frank Guerin. Compressing context to enhance inference
 644 efficiency of large language models, 2023. URL <https://arxiv.org/abs/2310.06201>.
 645

646 Yuhong Li, Yingbing Huang, Bowen Yang, Bharat Venkitesh, Acyr Locatelli, Hanchen Ye, Tianle Cai,
 647 Patrick Lewis, and Deming Chen. Snapkv: Llm knows what you are looking for before generation,
 648 2024b. URL <https://arxiv.org/abs/2404.14469>.
 649

650 Zhiyu Li, Shichao Song, Hanyu Wang, Simin Niu, Ding Chen, Jiawei Yang, Chenyang Xi, Huayi
 651 Lai, Jihao Zhao, Yezhaohui Wang, et al. Memos: An operating system for memory-augmented
 652 generation (mag) in large language models. *arXiv preprint arXiv:2505.22101*, 2025b. URL
 653 <https://arxiv.org/abs/2505.22101>.
 654

648 Zhiyu Li, Shichao Song, Chenyang Xi, Hanyu Wang, Chen Tang, Simin Niu, Ding Chen, Jiawei
 649 Yang, Chunyu Li, Qingchen Yu, Jihao Zhao, Yezhaohui Wang, Peng Liu, Zehao Lin, Pengyuan
 650 Wang, Jiahao Huo, Tianyi Chen, Kai Chen, Kehang Li, Zhen Tao, Junpeng Ren, Huayi Lai,
 651 Hao Wu, Bo Tang, Zhenren Wang, Zhaoxin Fan, Ningyu Zhang, Linfeng Zhang, Junchi Yan,
 652 Mingchuan Yang, Tong Xu, Wei Xu, Huajun Chen, Haofeng Wang, Hongkang Yang, Wentao
 653 Zhang, Zhi-Qin John Xu, Siheng Chen, and Feiyu Xiong. Memos: A memory os for ai system.
 654 *arXiv preprint arXiv:2507.03724*, 2025c. URL <https://arxiv.org/abs/2507.03724>.

655 Nelson F. Liu, Kevin Lin, John Hewitt, Ashwin Paranjape, Michele Bevilacqua, Fabio Petroni,
 656 and Percy Liang. Lost in the middle: How language models use long contexts, 2023a. URL
 657 <https://arxiv.org/abs/2307.03172>.

658 Zichang Liu, Aditya Desai, Fangshuo Liao, Weitao Wang, Victor Xie, Zhaozhuo Xu, Anastasios
 659 Kyrillidis, and Anshumali Shrivastava. Scissorhands: Exploiting the persistence of importance
 660 hypothesis for llm kv cache compression at test time. *Advances in Neural Information Processing
 661 Systems*, 36:52342–52364, 2023b.

662 Enzhe Lu, Zhejun Jiang, Jingyuan Liu, Yulun Du, Tao Jiang, Chao Hong, Shaowei Liu, Weiran He,
 663 Enming Yuan, Yuzhi Wang, Zhiqi Huang, Huan Yuan, Suting Xu, Xinran Xu, Guokun Lai, Yanru
 664 Chen, Huabin Zheng, Junjie Yan, Jianlin Su, Yuxin Wu, Neo Y. Zhang, Zhilin Yang, Xinyu Zhou,
 665 Mingxing Zhang, and Jiezhong Qiu. Moba: Mixture of block attention for long-context llms, 2025.
 666 URL <https://arxiv.org/abs/2502.13189>.

667 Aman Madaan, Niket Tandon, Prakhar Gupta, Skyler Hallinan, Luyu Gao, Sarah Wiegreffe, Uri Alon,
 668 Nouha Dziri, Shrimai Prabhumoye, Yiming Yang, Shashank Gupta, Bodhisattwa Prasad Majumder,
 669 Katherine Hermann, Sean Welleck, Amir Yazdanbakhsh, and Peter Clark. Self-refine: Iterative
 670 refinement with self-feedback. In *Advances in Neural Information Processing Systems*, 2023. doi:
 671 10.48550/arXiv.2303.17651.

672 OpenAI. Introducing GPT-4.1 in the API. <https://openai.com/index/gpt-4-1/>, April
 673 2025. Accessed: 2025-08-05.

674 Charles Packer, Sarah Wooders, Kevin Lin, Vivian Fang, Shishir G. Patil, Ion Stoica, and Joseph E.
 675 Gonzalez. Memgpt: Towards llms as operating systems, 2024. URL <https://arxiv.org/abs/2310.08560>.

676 Zhuoshi Pan, Qianhui Wu, Huiqiang Jiang, Menglin Xia, Xufang Luo, Jue Zhang, Qingwei Lin, Victor
 677 Rühle, Yuqing Yang, Chin-Yew Lin, H. Vicky Zhao, Lili Qiu, and Dongmei Zhang. Llmlingua-
 678 2: Data distillation for efficient and faithful task-agnostic prompt compression, 2024. URL
 679 <https://arxiv.org/abs/2403.12968>.

680 Bhargavi Paranjape, Scott Lundberg, Sameer Singh, Hannaneh Hajishirzi, Luke Zettlemoyer, and
 681 Marco Tulio Ribeiro. Art: Automatic multi-step reasoning and tool-use for large language models,
 682 2023. URL <https://arxiv.org/abs/2303.09014>.

683 Shishir G. Patil, Tianjun Zhang, Xin Wang, and Joseph E. Gonzalez. Gorilla: Large language model
 684 connected with massive apis, 2023. URL <https://arxiv.org/abs/2305.15334>.

685 Bowen Peng, Jeffrey Quesnelle, Honglu Fan, and Enrico Shippole. Yarn: Efficient context window
 686 extension of large language models, 2023. URL <https://arxiv.org/abs/2309.00071>.

687 Timo Schick, Jane Dwivedi-Yu, Roberto Dessì, Roberta Raileanu, Maria Lomeli, Luke Zettlemoyer,
 688 Nicola Cancedda, and Thomas Scialom. Toolformer: Language models can teach themselves to
 689 use tools, 2023. URL <https://arxiv.org/abs/2302.04761>.

690 Zhihong Shao, Peiyi Wang, Qihao Zhu, Runxin Xu, Junxiao Song, Xiao Bi, Haowei Zhang,
 691 Mingchuan Zhang, Y. K. Li, Y. Wu, and Daya Guo. Deepseekmath: Pushing the limits of
 692 mathematical reasoning in open language models, 2024. URL <https://arxiv.org/abs/2402.03300>.

693 Noah Shinn, Federico Cassano, Ashwin Gopinath, Karthik R. Narasimhan, and Shunyu Yao. Re-
 694 flexion: Language agents with verbal reinforcement learning. In *Advances in Neural Information
 695 Processing Systems*, 2023. doi: 10.48550/arXiv.2303.11366.

702 Mitchell Stern, William Chan, Jamie Kiros, and Jakob Uszkoreit. Insertion transformer: Flexible
 703 sequence generation via insertion operations. In *Proceedings of the 36th International Conference*
 704 *on Machine Learning*, volume 97 of *Proceedings of Machine Learning Research*, pp. 5976–5985.
 705 PMLR, 2019. URL <https://proceedings.mlr.press/v97/stern19a.html>.

706 Jianlin Su, Yu Lu, Shengfeng Pan, Ahmed Murtadha, Bo Wen, and Yunfeng Liu. Roformer: Enhanced
 707 transformer with rotary position embedding, 2023. URL <https://arxiv.org/abs/2104.09864>.

708 Mirac Suzgun, Mert Yuksekgonul, Federico Bianchi, Dan Jurafsky, and James Zou. Dynamic
 709 cheatsheet: Test-time learning with adaptive memory, 2025. URL <https://arxiv.org/abs/2504.07952>.

710 5 Team, Aohan Zeng, Xin Lv, Qinkai Zheng, Zhenyu Hou, Bin Chen, Chengxing Xie, Cunxiang
 711 Wang, Da Yin, Hao Zeng, Jiajie Zhang, Kedong Wang, Lucen Zhong, Mingdao Liu, Rui Lu, Shulin
 712 Cao, Xiaohan Zhang, Xuancheng Huang, Yao Wei, Yean Cheng, Yifan An, Yilin Niu, Yuanhao
 713 Wen, Yushi Bai, Zhengxiao Du, Zihan Wang, Zilin Zhu, Bohan Zhang, Bosi Wen, Bowen Wu,
 714 Bowen Xu, Can Huang, Casey Zhao, Changpeng Cai, Chao Yu, Chen Li, Chendi Ge, Chenghua
 715 Huang, Chenhui Zhang, Chenxi Xu, Chenzheng Zhu, Chuang Li, Congfeng Yin, Daoyan Lin,
 716 Dayong Yang, Dazhi Jiang, Ding Ai, Erle Zhu, Fei Wang, Gengzheng Pan, Guo Wang, Hailong
 717 Sun, Haitao Li, Haiyang Li, Haiyi Hu, Hanyu Zhang, Hao Peng, Hao Tai, Haoke Zhang, Haoran
 718 Wang, Haoyu Yang, He Liu, He Zhao, Hongwei Liu, Hongxi Yan, Huan Liu, Hui long Chen, Ji Li,
 719 Jiajing Zhao, Jiamin Ren, Jian Jiao, Jiani Zhao, Jianyang Yan, Jiaqi Wang, Jiayi Gui, Jiayue Zhao,
 720 Jie Liu, Jijie Li, Jing Li, Jing Lu, Jingsen Wang, Jingwei Yuan, Jingxuan Li, Jingzhao Du, Jinhua
 721 Du, Jinxin Liu, Junkai Zhi, Junli Gao, Ke Wang, Lekang Yang, Liang Xu, Lin Fan, Lindong Wu,
 722 Lintao Ding, Lu Wang, Man Zhang, Minghao Li, Minghuan Xu, Mingming Zhao, Mingshu Zhai,
 723 Pengfan Du, Qian Dong, Shangde Lei, Shangqing Tu, Shangtong Yang, Shaoyou Lu, Shijie Li,
 724 Shuang Li, Shuang-Li, Shuxun Yang, Sibo Yi, Tianshu Yu, Wei Tian, Weihan Wang, Wenbo Yu,
 725 Weng Lam Tam, Wenjie Liang, Wentao Liu, Xiao Wang, Xiaohan Jia, Xiaotao Gu, Xiaoying Ling,
 726 Xin Wang, Xing Fan, Xingru Pan, Xinyuan Zhang, Xinze Zhang, Xiuqing Fu, Xunkai Zhang, Yabo
 727 Xu, Yandong Wu, Yida Lu, Yidong Wang, Yilin Zhou, Yiming Pan, Ying Zhang, Yingli Wang,
 728 Yingru Li, Yinpei Su, Yipeng Geng, Yitong Zhu, Yongkun Yang, Yuhang Li, Yuhao Wu, Yujiang
 729 Li, Yunan Liu, Yunqing Wang, Yuntao Li, Yuxuan Zhang, Zezhen Liu, Zhen Yang, Zhengda Zhou,
 730 Zhongpei Qiao, Zhuoer Feng, Zhuorui Liu, Zichen Zhang, Zihan Wang, Zijun Yao, Zikang Wang,
 731 Ziqiang Liu, Ziwei Chai, Zixuan Li, Zuodong Zhao, Wenguang Chen, Jidong Zhai, Bin Xu, Minlie
 732 Huang, Hongning Wang, Juanzi Li, Yuxiao Dong, and Jie Tang. Glm-4.5: Agentic, reasoning, and
 733 coding (arc) foundation models, 2025a. URL <https://arxiv.org/abs/2508.06471>.

734 Kimi Team, Yifan Bai, Yiping Bao, Guanduo Chen, Jiahao Chen, Ningxin Chen, Ruijue Chen,
 735 Yanru Chen, Yuankun Chen, Yutian Chen, Zhuofu Chen, Jialei Cui, Hao Ding, Mengnan Dong,
 736 Angang Du, Chenzhuang Du, Dikang Du, Yulun Du, Yu Fan, Yichen Feng, Kelin Fu, Bofei Gao,
 737 Hongcheng Gao, Peizhong Gao, Tong Gao, Xinran Gu, Longyu Guan, Haiqing Guo, Jianhang
 738 Guo, Hao Hu, Xiaoru Hao, Tianhong He, Weiran He, Wenyang He, Chao Hong, Yangyang Hu,
 739 Zhenxing Hu, Weixiao Huang, Zhiqi Huang, Zihao Huang, Tao Jiang, Zhejun Jiang, Xinyi Jin,
 740 Yongsheng Kang, Guokun Lai, Cheng Li, Fang Li, Haoyang Li, Ming Li, Wentao Li, Yanhao
 741 Li, Yiwei Li, Zhaowei Li, Zheming Li, Hongzhan Lin, Xiaohan Lin, Zongyu Lin, Chengyin
 742 Liu, Chenyu Liu, Hongzhang Liu, Jingyuan Liu, Junqi Liu, Liang Liu, Shaowei Liu, T. Y. Liu,
 743 Tianwei Liu, Weizhou Liu, Yangyang Liu, Yibo Liu, Yiping Liu, Yue Liu, Zhengying Liu, Enzhe
 744 Lu, Lijun Lu, Shengling Ma, Xinyu Ma, Yingwei Ma, Shaoguang Mao, Jie Mei, Xin Men, Yibo
 745 Miao, Siyuan Pan, Yebo Peng, Ruoyu Qin, Bowen Qu, Zeyu Shang, Lidong Shi, Shengyuan
 746 Shi, Feifan Song, Jianlin Su, Zhengyuan Su, Xinjie Sun, Flood Sung, Heyi Tang, Jiawen Tao,
 747 Qifeng Teng, Chensi Wang, Dinglu Wang, Feng Wang, Haiming Wang, Jianzhou Wang, Jiaxing
 748 Wang, Jinhong Wang, Shengjie Wang, Shuyi Wang, Yao Wang, Yejie Wang, Yiqin Wang, Yuxin
 749 Wang, Yuzhi Wang, Zhaoji Wang, Zhengtao Wang, Zhexu Wang, Chu Wei, Qianqian Wei, Wenhao
 750 Wu, Xingzhe Wu, Yuxin Wu, Chenjun Xiao, Xiaotong Xie, Weimin Xiong, Boyu Xu, Jing Xu,
 751 Jinjing Xu, L. H. Xu, Lin Xu, Suting Xu, Weixin Xu, Xinran Xu, Yangchuan Xu, Ziyao Xu, Junjie
 752 Yan, Yuzi Yan, Xiaofei Yang, Ying Yang, Zhen Yang, Zhilin Yang, Zonghan Yang, Haotian Yao,
 753 Xingcheng Yao, Wenjie Ye, Zhuorui Ye, Bohong Yin, Longhui Yu, Enming Yuan, Hongbang Yuan,
 754 Mengjie Yuan, Haobing Zhan, Dehao Zhang, Hao Zhang, Wanlu Zhang, Xiaobin Zhang, Yangkun
 755 Zhang, Yizhi Zhang, Yongting Zhang, Yu Zhang, Yutao Zhang, Zheng Zhang,

756 Haotian Zhao, Yikai Zhao, Huabin Zheng, Shaojie Zheng, Jianren Zhou, Xinyu Zhou, Zaida Zhou,
 757 Zhen Zhu, Weiyu Zhuang, and Xinxing Zu. Kimi k2: Open agentic intelligence, 2025b. URL
 758 <https://arxiv.org/abs/2507.20534>.

759 Runchu Tian, Yanghao Li, Yuepeng Fu, Siyang Deng, Qinyu Luo, Cheng Qian, Shuo Wang, Xin
 760 Cong, Zhong Zhang, Yesai Wu, Yankai Lin, Huadong Wang, and Xiaojiang Liu. Distance
 761 between relevant information pieces causes bias in long-context llms, 2025. URL <https://arxiv.org/abs/2410.14641>.

762 Kiran Vodrahalli, Santiago Ontanon, Nilesh Tripuraneni, Kelvin Xu, Sanil Jain, Rakesh Shivanna,
 763 Jeffrey Hui, Nishanth Dikkala, Mehran Kazemi, Bahare Fatemi, Rohan Anil, Ethan Dyer, Siamak
 764 Shakeri, Roopali Vij, Harsh Mehta, Vinay Ramasesh, Quoc Le, Ed Chi, Yifeng Lu, Orhan Firat,
 765 Angeliki Lazaridou, Jean-Baptiste Lespiau, Nithya Attaluri, and Kate Olszewska. Michelangelo:
 766 Long context evaluations beyond haystacks via latent structure queries, 2024a. URL <https://arxiv.org/abs/2409.12640>.

767 Kiran Vodrahalli, Santiago Ontanon, Nilesh Tripuraneni, Kelvin Xu, Sanil Jain, Rakesh Shivanna,
 768 Jeffrey Hui, Nishanth Dikkala, Mehran Kazemi, Bahare Fatemi, Rohan Anil, Ethan Dyer, Siamak
 769 Shakeri, Roopali Vij, Harsh Mehta, Vinay Ramasesh, Quoc Le, Ed Chi, Yifeng Lu, Orhan Firat,
 770 Angeliki Lazaridou, Jean-Baptiste Lespiau, Nithya Attaluri, and Kate Olszewska. Michelangelo:
 771 Long context evaluations beyond haystacks via latent structure queries, 2024b. URL <https://arxiv.org/abs/2409.12640>.

772 Chupei Wang and Jiaqiui Vince Sun. Unable to forget: Proactive interference reveals working memory
 773 limits in llms beyond context length, 2025. URL <https://arxiv.org/abs/2506.08184>.

774 Yu Wang and Xi Chen. Mirix: Multi-agent memory system for llm-based agents, 2025. URL
 775 <https://arxiv.org/abs/2507.07957>.

776 Yu Wang, Yifan Gao, Xiusi Chen, Haoming Jiang, Shiyang Li, Jingfeng Yang, Qingyu Yin, Zheng Li,
 777 Xian Li, Bing Yin, Jingbo Shang, and Julian McAuley. Memoryllm: Towards self-updatable large
 778 language models, 2024. URL <https://arxiv.org/abs/2402.04624>.

779 Hao Wen, Yifan Su, Feifei Zhang, Yunxin Liu, Yunhao Liu, Ya-Qin Zhang, and Yuanchun Li.
 780 Parathinker: Native parallel thinking as a new paradigm to scale llm test-time compute. 2025. doi:
 781 10.48550/arXiv.2509.04475.

782 Guangxuan Xiao, Yuandong Tian, Beidi Chen, Song Han, and Mike Lewis. Efficient streaming lan-
 783 guage models with attention sinks, 2024. URL <https://arxiv.org/abs/2309.17453>.

784 Fangyuan Xu, Weijia Shi, and Eunsol Choi. Recomp: Improving retrieval-augmented lms with
 785 compression and selective augmentation, 2023. URL <https://arxiv.org/abs/2310.04408>.

786 Hongkang Yang, Lin Zehao, Wang Wenjin, Hao Wu, Li Zhiyu, Bo Tang, Wei Wen-
 787 qiang, Jinbo Wang, Tang Zeyun, Shichao Song, Chenyang Xi, Yu Yu, Chen Kai, Feiyu
 788 Xiong, Linpeng Tang, and E Weinan. Memory³: Language modeling with explicit
 789 memory. *Journal of Machine Learning*, 3(3):300–346, 2024. ISSN 2790-2048. doi:
 790 <https://doi.org/10.4208/jml.240708>. URL <https://global-sci.com/article/91443/memory3-Language-modeling-with-explicit-memory>.

791 Shunyu Yao, Dian Yu, Jeffrey Zhao, Izhak Shafran, Thomas L. Griffiths, Yuan Cao, and Karthik
 792 Narasimhan. Tree of thoughts: Deliberate problem solving with large language models. 2023a.
 793 doi: 10.48550/arXiv.2305.10601.

794 Shunyu Yao, Jeffrey Zhao, Dian Yu, Nan Du, Izhak Shafran, Karthik Narasimhan, and Yuan Cao.
 795 React: Synergizing reasoning and acting in language models, 2023b. URL <https://arxiv.org/abs/2210.03629>.

796 Hongli Yu, Tinghong Chen, Jiangtao Feng, Jiangjie Chen, Weinan Dai, Qiying Yu, Ya-Qin Zhang,
 797 Wei-Ying Ma, Jingjing Liu, Mingxuan Wang, and Hao Zhou. Memagent: Reshaping long-context
 798 llm with multi-conv rl-based memory agent, 2025. URL <https://arxiv.org/abs/2507.02259>.

810 Jingyang Yuan, Huazuo Gao, Damai Dai, Junyu Luo, Liang Zhao, Zhengyan Zhang, Zhenda Xie,
811 Y. X. Wei, Lean Wang, Zhiping Xiao, Yuqing Wang, Chong Ruan, Ming Zhang, Wenfeng Liang,
812 and Wangding Zeng. Native sparse attention: Hardware-aligned and natively trainable sparse
813 attention, 2025. URL <https://arxiv.org/abs/2502.11089>.

814 Jenny Zhang, Shengran Hu, Cong Lu, Robert Lange, and Jeff Clune. Darwin godel machine: Open-
815 ended evolution of self-improving agents, 2025a. URL <https://arxiv.org/abs/2505.22954>.

816 Yanzhao Zhang, Mingxin Li, Dingkun Long, Xin Zhang, Huan Lin, Baosong Yang, Pengjun
817 Xie, An Yang, Dayiheng Liu, Junyang Lin, Fei Huang, and Jingren Zhou. Qwen3 embed-
818 ding: Advancing text embedding and reranking through foundation models, 2025b. URL
819 <https://arxiv.org/abs/2506.05176>.

820 Chujie Zheng, Shixuan Liu, Mingze Li, Xiong-Hui Chen, Bowen Yu, Chang Gao, Kai Dang, Yuqiong
821 Liu, Rui Men, An Yang, Jingren Zhou, and Junyang Lin. Group sequence policy optimization,
822 2025. URL <https://arxiv.org/abs/2507.18071>.

823 Yang Zhou, Hongyi Liu, Zhuoming Chen, Yuandong Tian, and Beidi Chen. Gsm-infinite: How do
824 your llms behave over infinitely increasing context length and reasoning complexity?, 2025. URL
825 <https://arxiv.org/abs/2502.05252>.

826
827
828
829
830
831
832
833
834
835
836
837
838
839
840
841
842
843
844
845
846
847
848
849
850
851
852
853
854
855
856
857
858
859
860
861
862
863

864 **A USE OF LARGE LANGUAGE MODELS**
865866 Large language models were used as a general-purpose assist tool during the writing process of this
867 paper, primarily for grammar checking and improving clarity of technical descriptions. All scientific
868 ideas, experimental design, and analysis were conducted by the authors. The LLMs did not contribute
869 to research ideation or core scientific content. The authors take full responsibility for all content in
870 this paper, including its accuracy and originality.871
872 **B RELATED WORK**
873874 **Long-Context Processing, Memory, and Evaluation** Effectively processing long contexts remains
875 a critical challenge for LLMs. Early efforts focused on expanding context windows through archi-
876 tectural improvements (Su et al., 2023; Chen et al., 2023; Beltagy et al., 2020) and sparse attention
877 mechanisms (Yuan et al., 2025; Gao et al., 2025; Lu et al., 2025). Subsequently, a substantial body of
878 work sought to further optimize performance by augmenting LLMs with external memory systems,
879 employing comprehensive memory architectures and multi-agent frameworks to overcome context
880 limitations (Yang et al., 2024; Li et al., 2025b; Wang & Chen, 2025; Chhikara et al., 2025; Packer
881 et al., 2024; Wang et al., 2024; Yu et al., 2025). The push for longer and more complex context
882 processing led to the development of specialized evaluation benchmarks, such as NIAH (Kamradt,
883 2023), NeedleBench (Li et al., 2025a), RULER (Hsieh et al., 2024a), LongBench-v2 (Bai et al., 2025),
884 MRCR (Vodrahalli et al., 2024b), and PI-LLM (Wang & Sun, 2025). These benchmarks were
885 instrumental in revealing that despite architectural and memory enhancements, modern LLMs still
886 perform poorly on information-sparse tasks. Among these, work such as PI-LLM further identified a
887 deeper reason for this phenomenon: proactive interference, where earlier information in the context
888 disrupts the processing of later, more relevant content (Wang & Sun, 2025). These documented
889 failures on information-sparse tasks, coupled with the diagnosis of proactive interference, provide a
890 strong motivation for our approach of active context management. Unlike external memory solutions
891 that focus on storage and retrieval, or sparse attention that modifies token processing patterns, our
892 complementary method provides the model with explicit tools to selectively retain, compress, or ig-
893 nore information directly within its working memory, thereby mitigating interference while operating
894 alongside existing architectural enhancements.895 **Tool-Augmented Language Models** The integration of external tools to augment LLM capabilities
896 is a burgeoning field of research, designed to overcome inherent model limitations such as knowledge
897 cutoffs, hallucination, and weak mathematical reasoning. Pioneering work in this area has largely
898 followed two paradigms. On one hand, models like Toolformer (Schick et al., 2023) demonstrate
899 that LLMs can be fine-tuned to learn when and how to call external APIs, seamlessly incorporating
900 their outputs into the generation process. On the other hand, prompting-based frameworks like
901 ReAct (Yao et al., 2023b) show that LLMs can synergize chain-of-thought reasoning with tool
902 use in a zero-shot manner, interleaving thought, action, and observation steps to solve complex
903 tasks. Subsequent research has focused on improving the reliability and scope of tool use, with
904 work like Gorilla (Patil et al., 2023) developing models specialized for accurate API invocation, and
905 frameworks like ART (Paranjape et al., 2023) creating programmatic pipelines for tool-augmented
906 multi-step reasoning. However, a common thread in this existing literature is the focus on using
907 tools to interact with the *external* world—accessing calculators, search engines, or code interpreters.
908 **Sculptor** diverges from this trend by proposing a novel class of tools for *internal* context management.
909 Instead of augmenting the LLM with external knowledge, we empower it with cognitive tools to
910 actively curate its own working memory. This positions our work as complementary to existing
911 tool-use research. Our approach directly targets cognitive bottlenecks like proactive interference,
912 rather than solely addressing knowledge or computational limitations.913 **From External Compression to Internal Context Curation** A complementary line of research
914 focuses on reducing the computational and memory burden of long contexts through **intelligent**
915 **compression** and **selection mechanisms**. The LLMLingua series (Jiang et al., 2023; 2024a; Pan
916 et al., 2024) pioneered the use of smaller models as compressors, performing extractive compression
917 to remove task-irrelevant sentences and phrases while preserving information density. LongLLM-
918 Lingua (Jiang et al., 2024a) further advanced this approach with question-aware coarse-to-fine
919 compression and dynamic compression ratios, achieving significant improvements on long-context

benchmarks. Similarly, Selective Context (Li et al., 2023) formalizes context selection as a relevance-based filtering problem for reading comprehension tasks. **At the inference level**, several methods optimize KV cache management to handle longer sequences more efficiently. StreamingLLM (Xiao et al., 2024) introduces attention sink mechanisms for online processing of extremely long inputs, while Scissorhands (Liu et al., 2023b) selectively retains only the KV pairs that will be referenced in future computations. More recent work like SnapKV (Li et al., 2024b) and KVQuant (Hooper et al., 2025) focus on pre-computation importance estimation and low-bit quantization respectively to achieve memory-efficient inference. While these compression and selection methods effectively reduce computational overhead, they share a fundamental limitation: the compression decisions are made externally to the reasoning process, either by separate models or fixed heuristics. This can lead to information loss that the primary LLM might deem crucial for its reasoning chain. In contrast, **Sculptor** enables the LLM itself to make context management decisions dynamically based on its internal reasoning state, ensuring that compression and selection align with the model’s cognitive needs rather than external approximations.

Revisable Generation and Editable Thought Processes Autoregressive decoding makes early errors “sticky” causing later tokens to amplify rather than fix them. Proactive interference tests show that retrieval accuracy degrades as semantically related but obsolete updates accumulate, underscoring the cost of an immutable context (Wang & Sun, 2025). Causally, pruning failed reasoning branches—or removing their surface forms from the visible history—immediately improves subsequent correctness, indicating the harmful persistence of erroneous traces (Feng et al., 2025). To mitigate this prefix lock-in, one line of work explores parallel or branched reasoning, such as the search-based Tree of Thoughts and the native parallelism in ParaThinker, which reduces “tunnel vision” at a small latency overhead (Yao et al., 2023a; Wen et al., 2025). A more fundamental approach alters the generation process itself, making outputs inherently revisable. This includes models that perform discrete edits, like iterative refinement via masking (Ghazvininejad et al., 2019) or sequence modification through insertion and deletion operations (Stern et al., 2019; Gu et al., 2019). Another family of non-autoregressive paradigms, such as diffusion LMs, enables global backtracking by denoising entire sequences in parallel (Li et al., 2022; Austin et al., 2021). Complementing these architectural shifts, test-time self-revision loops like Self-Refine and Reflexion demonstrate that lightweight edits to intermediate outputs reliably improve final solutions (Madaan et al., 2023; Shinn et al., 2023). Collectively, these findings build a strong case for equipping models with mechanisms to remove, rewrite, or compress their working context during reasoning—rather than merely appending tokens—so they can correct course instead of being trapped by early errors.

C BASELINE MODEL PERFORMANCE

We evaluate M3 across standard benchmarks and compare it with both smaller-scale models (Qwen3-8B, Qwen3-14B) and frontier models to establish baseline capabilities before ACM training. The results are presented in Table 3. Despite being a 13B model, M3 demonstrates exceptional tool-use performance, achieving 61.0% on Tau2-retail (Barres et al., 2025) (vs. 27.9% for Qwen3-8B), 61.8% on AceBench (Chen et al., 2025) (vs. 24.3% for Qwen3-8B), and 32.0% on SWE-bench Verified (vs. 3.3% for Qwen3-8B). This strong tool-calling foundation makes it particularly suitable for demonstrating ACM effectiveness. Additionally, we include GLM-4.5-Air benchmark scores in Table 3 to provide comprehensive baseline comparisons for the open-source model used in our main experiments (Table 2). Benchmark results for GLM-4.5-Air are reported from their technical report (Team et al., 2025a). Benchmark results for DeepSeek-V3, GPT-4.1, and Claude-4-Sonnet (excluding NeedleBench-MRS and PI-LLM) are taken from the Kimi-K2 technical report (Team et al., 2025b).

For Qwen3-8B and Qwen3-14B models, we followed the official documentation¹ to enable 128K context length support through RoPE scaling (Su et al., 2023) with the YaRN method (Peng et al., 2023), using a scaling factor of 4.0 to extend from their original 32K context window to 128K tokens. This configuration was necessary for fair comparison on long-context benchmarks.

¹<https://qwen.readthedocs.io/en/latest/deployment/vllm.html>

972 Table 3: Performance of M3 (13B parameters) compared to other models on standard benchmarks.
 973 Left: smaller-scale models (8B-14B). Right: frontier models. M3 demonstrates particularly strong
 974 tool-use capabilities (Tau2, AceBench) and coding performance (SWE-bench Verified).

Benchmark	Qwen3-8B	Qwen3-14B	M3	GLM-4.5-Air	Kimi-K2	DeepSeek-V3	GPT-4.1	Claude-4-Sonnet
Coding Tasks								
LiveCodeBench v6 (Pass@1)								
978 MultiPL-E (Pass@1)	50.2	51.8	25.1	70.7	53.7	46.9	44.7	48.5
979 SWE-bench Verified (Pass@1)	70.4	77.0	72.4	—	85.7	83.1	86.7	88.6
Tool Use Tasks								
980 Tau2 retail (Avg@4)	27.9	36.2	61.0	77.9	70.6	69.1	74.8	75.0
981 Tau2 airline (Avg@4)	18.0	39.0	54.0	60.8	56.5	39.0	54.5	55.5
982 AceBench (Acc.)	24.3	23.7	61.8	76.4	76.5	72.7	80.1	76.2
Math & STEM Tasks								
983 MATH-500 (Acc.)	92.2	95.4	80.2	98.1	97.4	94.0	92.4	94.0
984 AIME 2024 (Avg@64)	60.9	60.8	17.7	89.4	69.6	59.4	46.5	43.4
985 GPQA-Diamond (Avg@8)	53.0	58.1	45.2	75.0	75.1	68.4	66.3	70.0
General Tasks								
986 MMLU (EM)	80.1	85.0	78.6	87.4	89.5	89.4	90.4	91.5
987 MMLU-Pro (EM)	74.5	77.5	65.2	81.4	81.1	81.2	81.8	83.7
988 IFEval (Prompt Strict)	34.9	35.5	77.1	86.3	89.8	81.1	88.0	87.6
989 SimpleQA (Correct)	6.7	8.8	7.4	14.5	31.0	27.7	42.3	15.9

D EVALUATION DETAILS

D.1 BENCHMARK-SPECIFIC SYSTEM PROMPTS

995 As described in Section 4.1, we employed prompt engineering to enhance tool utilization capabilities
 996 across frontier models. The system prompts presented here are the final optimized versions used
 997 in our zero-shot evaluation for PI-LLM and NeedleBench benchmarks. These benchmark-specific
 998 prompts significantly improved Claude-4-Sonnet’s performance, demonstrating how targeted prompt
 999 optimization can unlock more effective **Sculptor** tool usage patterns.

System Prompt for PI-LLM Benchmark

System Prompt:

1003 You are an intelligent assistant specialized for PI-LLM (Proactive Interference) testing. Your
 1004 task is to track continuous updates to multiple key-value pairs and accurately remember the
 1005 latest value for each key amidst substantial interference information.
 1006 Remember: First use the fragment_context tool to split the long text into multiple fragments,
 1007 then use fold_fragment to fold unimportant, earlier key-value updates, allowing you to
 1008 concentrate on the final updates. The recommended approach is to divide the entire update
 1009 stream into multiple fragments (e.g., ten fragments), then keep only the last two or three
 1010 fragments while folding the rest. This strategy enables focus on the current, most recent
 1011 content without being distracted by earlier information.

1013 Figure 7: System prompt for PI-LLM benchmark, designed to handle proactive interference through
 1014 strategic tool usage.

D.2 UNIFIED SYSTEM PROMPT

1019 The unified system prompt is used in our initial zero-shot evaluations and RL training experiments.
 1020 This minimal, general-purpose prompt provides only basic guidance about available capabilities
 1021 without prescriptive task-specific strategies. As described in Section 4.1, experiments with this
 1022 unified prompt revealed inherent challenges of unguided tool use, including suboptimal tool selection
 1023 patterns and insufficient execution depth. During RL training, the same prompt enables the model to
 1024 autonomously discover optimal tool usage patterns across diverse contexts, as shown in Figure 9.

1025 This approach ensures that the model learns generalizable context management strategies rather than
 memorizing task-specific patterns, leading to more robust performance across diverse long-context.

1026
1027

System Prompt for NeedleBench Multi-Needle Reasoning

1028

System Prompt:

1029

You are an agent skilled at analyzing family relationships between different people. You have "search_context" and "get_search_detail" tools. You excel at conducting chained searches for key information in long texts until you find complete information to reach your desired final answer.

1030

When searching for the oldest ancestor, ensure that every person name found has been verified through the search tools to confirm they truly have no higher-level ancestors before concluding your reasoning.

1031

1032

1033

1034

1035

1036

1037

1038

1039

1040

1041

1042

1043

1044

1045

1046

1047

1048

1049

1050

1051

1052

1053

1054

1055

1056

1057

1058

1059

1060

1061

1062

1063

1064

1065

1066

1067

1068

1069

1070

1071

1072

1073

1074

1075

1076

1077

1078

1079

Unified System Prompt

System Prompt:

You are a helpful assistant. You can autonomously manage your own context: fold irrelevant information, focus on useful details, summarize long texts to keep your context concise, and use search tools to find key information in large documents.

Figure 8: System prompt for NeedleBench Multi-Needle Reasoning, optimized for multi-hop retrieval tasks.

Figure 9: The unified general-purpose prompt used both in initial zero-shot evaluations (to understand natural tool interaction patterns) and in RL training (to enable autonomous learning of tool usage strategies without prescriptive guidance).

D.3 BENCHMARK DETAILS

We provide detailed configurations for the benchmarks used in our experiments:

NeedleBench Multi-Needle Reasoning: For efficiency while maintaining representativeness, we test with a fixed depth of 40%, as our tool-based approach shows minimal sensitivity to needle position within the context. We examine context lengths of 1k, 2k, 16k, 64k, and 128k tokens, with each configuration evaluated across 10 runs per dataset to ensure statistical significance. The multi-needle variant requires connecting 2, 3, 4, and 5 needles simultaneously, making it substantially more challenging than single-needle retrieval tasks.

Data Processing for Context Length Constraints: To ensure evaluation within our model's 128k context window, we apply minimal preprocessing. For MRCR, we filter out test samples exceeding 128k tokens. For LongBench v2, we truncate samples exceeding 128k tokens using our tokenizer.

D.4 BASELINE METHOD EVALUATION DETAILS: RAG, MEM0, AND MEMAGENT

We include three baseline approaches for long-context processing in our main results (see Table 2): retrieval-augmented generation (**RAG**) as a traditional long-context method, **Mem0** as a cross-session external memory system, and **MemAgent** as an inner working memory approach. All baselines are evaluated under a unified, lightweight interface that accepts plain strings or standard message arrays, without dataset-specific restructuring.

For **RAG**, we evaluate two retrieval approaches to represent both traditional and modern methods:

BM25-based RAG²: We adopt a BM25-only pipeline aligned with LongBench-style retrieval. The input is sentence-split with the same punctuation and length heuristics as common LongBench implementations, then chunked at 200 tokens. A pseudo query is formed by concatenating the first and last 500 tokens of the full context when an explicit query is not provided. Chunks are ranked

²<https://github.com/THUDM/LongBench/tree/main/LongBench/retrieval/BM25>

1080 by BM25 and concatenated from high to low until the accumulated length reaches ≈ 1500 tokens.
 1081 The system prompt constrains the model to answer strictly based on the retrieved context. This
 1082 BM25-only design avoids external dense embeddings and evaluates the model’s intrinsic ability to
 1083 reason over the retrieved snippets.

1084 **Embedding-based RAG:** We additionally evaluate dense retrieval using the Qwen3 embedding
 1085 model (Zhang et al., 2025b), a state-of-the-art text embedding model. The input is chunked similarly
 1086 at 200 tokens. For each chunk, we compute dense embeddings using the Qwen3 embedding model
 1087 and rank chunks by cosine similarity to the query embedding. The top-ranked chunks are concatenated
 1088 until reaching ≈ 1500 tokens, and the model generates answers based on the retrieved context. This
 1089 approach represents modern embedding-based RAG systems widely adopted in production settings.

1090 For **MemAgent**(Yu et al., 2025)³, we follow their implementation with iterative memory updates.
 1091 Extremely long inputs are first symmetrically trimmed to a maximum visible length of about 120 k
 1092 tokens to avoid one-sided truncation. The remaining text is processed in fixed 5 k-token chunks. At
 1093 each step the model updates an explicit "memory" that preserves previously useful information and
 1094 integrates newly relevant details from the current chunk; the final answer is generated using the last
 1095 memory along with the query. When no explicit query is given, we construct a short pseudo query
 1096 from the first and last 500 tokens of the source. Unless otherwise noted, defaults are: max context
 1097 length ≈ 120 k tokens, chunk size 5 k tokens, and maximum generation length 1024 tokens.

1098 For **Mem0**(Chhikara et al., 2025), we adapt the official implementation for long-context evalua-
 1099 tion. Since Mem0 is designed for cross-session user preference memory rather than single-session
 1100 document processing, we modify: (1) the fact extraction prompt to focus on document-relevant
 1101 information instead of user preferences, and (2) the chunking mechanism to include the query in each
 1102 5 k-token chunk, ensuring the memory LLM can extract question-relevant facts. Each question uses a
 1103 unique user ID to prevent memory interference across samples.

1104 These choices emphasize reproducibility and represent diverse approaches to long-context processing:
 1105 traditional and modern retrieval methods for RAG, cross-session external memory for Mem0, and
 1106 inner working memory for MemAgent. Detailed hyperparameters are reflected in the text above
 1107 rather than bespoke configuration tables to keep the protocol concise and focused.

1109 E DYNAMIC CONTEXT-AWARE TRAINING DATA COLLECTION

1111 Algorithm 1 presents our conditional trajectory collection algorithm with incremental loss assignment
 1112 for dynamic context-aware RL training. The algorithm identifies context-modifying tool calls and
 1113 creates separate training instances at each modification point, with incremental loss assignment to
 1114 prevent redundant learning across multiple trajectory snapshots.

1116 F TRAINING CONFIGURATION

1118 To ensure reproducibility and facilitate future research building upon our work, we provide the
 1119 detailed training hyperparameters and hardware configuration used for GSPO training in Table 4.
 1120 These settings represent the optimal configuration determined through extensive experimentation for
 1121 training Sculptor-M3-RL with dynamic context-aware capabilities.

1123 Table 4: GSPO training configuration.

1125 Training Hyperparameters		1126 Hardware & Parallelism	
Learning rate	1×10^{-6}	GPU type	NVIDIA H800 (80GB)
Training iterations	200	Total GPUs	128 (64 train, 64 rollout)
Clip ratio (lower)	0.0003	Tensor parallel (TP)	1
Clip ratio (upper)	0.0004	Pipeline parallel (PP)	4
KL penalty (α)	0.0	Context parallel (CP)	16
LM regularization	0.1	Data parallel (DP)	4
Optimizer	AdamW	Max sequence length	128k tokens

1133 ³<https://github.com/BytedTsinghua-SIA/MemAgent/blob/main/quickstart.py>

1134
 1135
 1136
 1137
 1138
 1139
 1140
 1141
 1142
 1143
 1144
 1145
 1146
 1147 **Algorithm 1** Conditional Trajectory Collection with Incremental Loss Assignment
 1148
 1149 **Require:** Initial query Q , complete interaction trajectory with assistant completions $\{C_i\}_{i=0}^n$ and
 1150 tool results $\{T_i\}_{i=0}^{n-1}$.
 1151 **Require:** Set of context-modifying tools \mathcal{T}_{ctx} (fragment, fold, summarize, restore operations).
 1152 **Ensure:** Training dataset \mathcal{D}_{train} containing (trajectory, loss_mask) pairs.
 1153 1: Initialize $\mathcal{D}_{train} \leftarrow \emptyset$
 1154 2: Initialize $trained_indices \leftarrow \emptyset$ \triangleright Track completion indices that have been assigned loss=1
 1155 3: **for** $i = 0$ **to** n **do**
 1156 4: Extract tool call a_i from completion C_i
 1157 5: **if** $a_i \in \mathcal{T}_{ctx}$ **or** $i = n$ **then** \triangleright Context modification or final completion
 1158 6: $trajectory \leftarrow [Q, C_0, T_0, C_1, T_1, \dots, C_i]$ \triangleright Create trajectory snapshot up to current point
 1159 7: **if** $i < n$ **then**
 1160 8: $trajectory \leftarrow trajectory + [T_i]$ \triangleright Include tool result if not final
 1161 9: **end if**
 1162 10: \triangleright Create incremental loss mask
 1163 11: Initialize $loss_mask$ with zeros for all elements in $trajectory$
 1164 12: **for** $j = 0$ **to** i **do**
 1165 13: **if** $j \notin trained_indices$ **then** \triangleright Only assign loss to new completions
 1166 14: $loss_mask[C_j] \leftarrow 1$ \triangleright Enable loss for completion C_j
 1167 15: $trained_indices \leftarrow trained_indices \cup \{j\}$
 1168 16: **end if**
 1169 17: **end if**
 1170 18: **end for**
 1171 19: $\mathcal{D}_{train} \leftarrow \mathcal{D}_{train} \cup \{(trajectory, loss_mask)\}$
 1172 20: **if** $a_i \in \mathcal{T}_{ctx}$ **then** \triangleright Update query for next iteration if context modified
 1173 21: $Q \leftarrow \text{ApplyToolEffect}(Q, a_i, T_i)$ \triangleright Apply context modification
 1174 22: **end if**
 1175 23: **end if**
 1176 24: **end for**
 1177 25: **return** \mathcal{D}_{train}
 1178
 1179
 1180
 1181
 1182
 1183
 1184
 1185
 1186
 1187

1188 **Reward Design.** Our reward function for GSPO training is defined as:
 1189

$$1190 \quad r(x, \tau) = \begin{cases} 1 & \text{if correct answer} \\ 1191 \quad -1 & \text{if format error or } n_{\text{tools}} > 20 \text{ or } |\tau| > 128k \text{ tokens} \\ 1192 \quad 0 & \text{otherwise} \\ 1193 \end{cases} \quad (4)$$

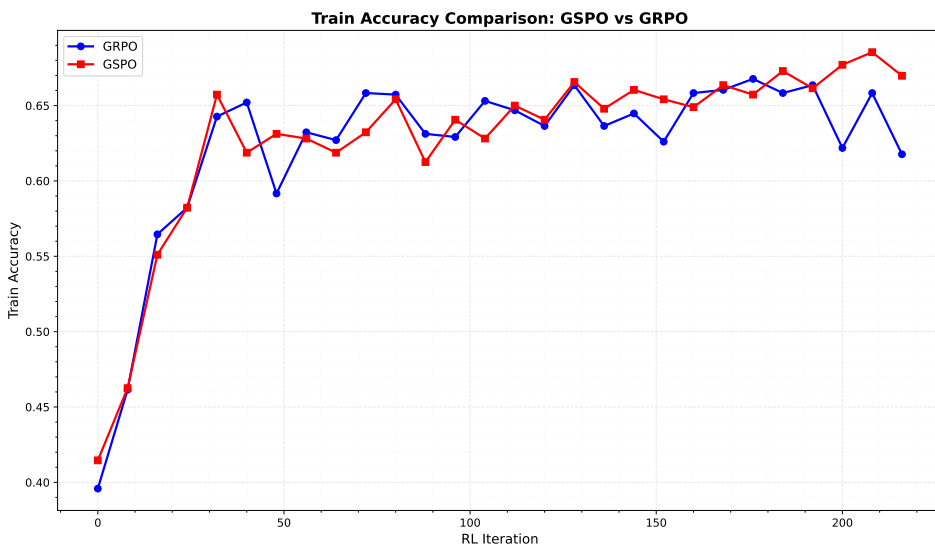
1194 This design encourages correct task completion while penalizing excessive tool usage, overly long
 1195 trajectories, and malformed outputs.
 1196

1197 G RL TRAINING DYNAMICS AND TOOL USAGE ANALYSIS

1200 This section provides detailed analysis of the reinforcement learning training process, including
 1201 training dynamics across iterations and the evolution of tool usage patterns.
 1202

1203 G.1 TRAINING ACCURACY COMPARISON: GSPO vs GRPO

1205 We compare two RL training approaches: GSPO (Group Sequence Policy Optimization) (Zheng
 1206 et al., 2025) adapted with our dynamic context-aware extensions, and GRPO (Group Relative Policy
 1207 Optimization) (Shao et al., 2024) as a baseline. Figure 10 shows the training accuracy curves across
 1208 RL iterations. Both methods demonstrate consistent learning progress, achieving comparable final
 1209 performance (66-67%). GSPO shows slightly more stable convergence during later training iterations,
 1210 validating our choice for the main experiments. The similar performance of both algorithms suggests
 1211 that our dynamic context-aware training framework is not tightly coupled to a specific RL algorithm
 1212 choice, demonstrating compatibility with different policy optimization methods. This indicates that
 1213 when given the same training data, the choice of specific RL algorithm has limited impact on final
 1214 results, with data quality and task design being more critical factors.
 1215



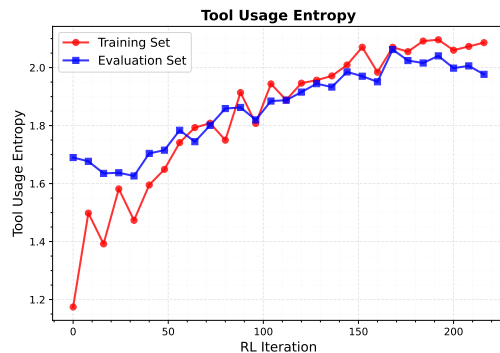
1233 Figure 10: Training accuracy comparison between GSPO and GRPO across RL iterations. Both
 1234 methods show steady improvement and achieve similar final performance.
 1235
 1236

1237 G.2 TOOL USAGE EVOLUTION DURING RL TRAINING

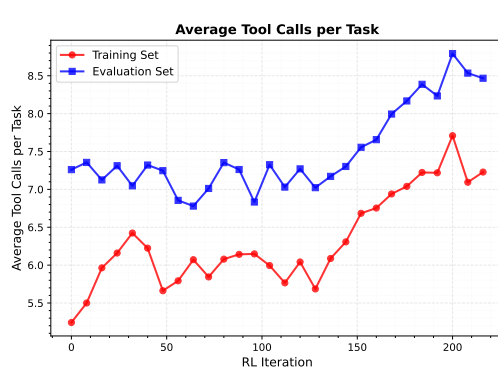
1238 To understand how the RL policy learns to use different tools, we analyze tool usage patterns across
 1239 training iterations. We examine both the overall diversity of tool usage (measured by entropy) and
 1240 specific tool call patterns on PI-LLM tasks, which require extensive context management through
 1241 folding and selective restoration of information.

1242 G.2.1 TOOL USAGE DIVERSITY AND INTENSITY
1243

1244 As RL training progresses, we observe two complementary trends in tool usage behavior. First, tool
1245 usage entropy increases substantially (training set: 1.17 to 2.09, +77.6%; evaluation set: 1.69 to
1246 1.98, +17.0%), indicating the policy learns to leverage a more diverse repertoire of tools based on
1247 task requirements. Second, the average number of tool calls per task increases from 7.26 to 8.47
1248 (+16.6%) on evaluation benchmarks, demonstrating more intensive and sophisticated use of available
1249 tools. Together, these patterns show that the policy evolves from relying on a few dominant tools to
1250 strategically employing the full range of capabilities (fold, restore, search, etc.) when needed, which
1251 is critical for robust performance across diverse long-context scenarios.



1252
1253
1254 Figure 11: Tool usage entropy across RL training
1255 iterations. The substantial increase indicates
1256 more diverse tool selection.
1257
1258
1259
1260
1261
1262
1263
1264



1265 Figure 12: Average tool calls per task across RL
1266 training iterations.
1267
1268
1269
1270
1271
1272
1273

G.2.2 TOOL CALL PATTERNS ON PI-LLM TASKS

1274 Figure 13 presents how the RL policy learns to balance compression and information preservation
1275 on PI-LLM tasks. Initially, the policy relies heavily on `fold_fragment` for context compression
1276 with minimal use of `restore_fragment` (0.052 calls per task). However, excessive folding can
1277 discard critical information, leading to accuracy degradation. Through RL training with accuracy-
1278 based rewards, the policy gradually learns to recover over-compressed useful information. The
1279 usage of `fold_fragment` increases from 4.85 to 7.08 calls per task (+45.8%), while critically,
1280 `restore_fragment` usage grows from 0.052 to 0.267 calls per task (+416.6%). More signifi-
1281 cantly, comparing early iterations (0-40) to late iterations (160-208), the average restore usage in-
1282 creases from 0.0746 to 0.2068, representing a **177.2% growth**. Notably, `summarize_fragment`
1283 remains near zero throughout training, indicating the policy intelligently recognizes that PI-LLM
1284 tasks involve truly irrelevant context that should be directly folded rather than summarized—a more
1285 efficient strategy when the discarded information is genuinely unnecessary. This learned restore
1286 behavior enables the model to achieve near-perfect performance on PI-LLM tasks, demon-
1287 strating that the RL policy successfully learns to proactively recover information when aggressive
1288 compression risks losing critical details.

1288 The substantial increase in restore usage during later training iterations directly addresses concerns
1289 about robustness to over-compression. Early in training, the policy predominantly uses folding
1290 without restoration, which can lead to information loss and accuracy drops. The accuracy-based
1291 reward signal drives the policy to discover that restoring over-compressed fragments can recover lost
1292 information and improve task performance. The simultaneous increase in both fold and restore usage
1293 indicates the policy learns to compress aggressively while developing safeguards through selective
1294 restoration. These patterns validate that our reversible tool design successfully enables the RL policy
1295 to learn robust context management strategies, ultimately achieving near-perfect accuracy on PI-LLM
by balancing compression efficiency with the ability to recover critical information when needed.

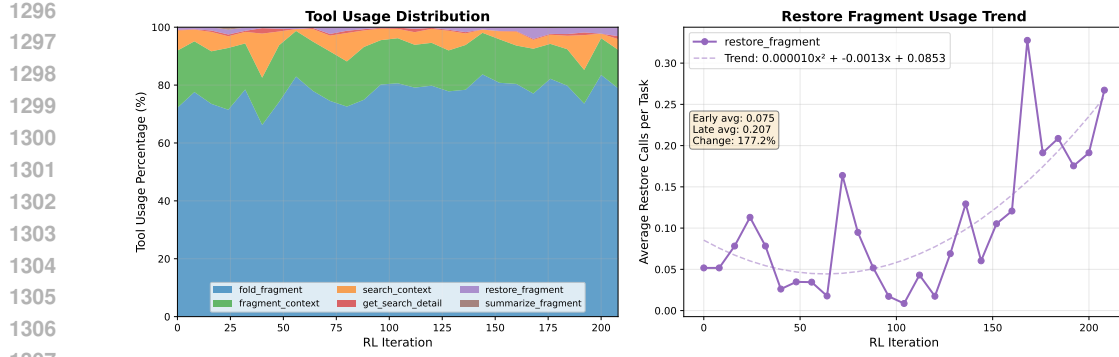


Figure 13: Tool usage evolution on PI-LLM tasks across RL training iterations. (Left) Percentage distribution showing restore_fragment’s relative proportion increasing over training, demonstrating more diverse tool usage. (Right) Absolute restore usage trend showing the average restore calls per task steadily increases, indicating the policy learns to proactively recover information when needed.

H SCULPTOR TOOL SUITE SCHEMAS

We provide the complete JSON schemas for all six core **Sculptor** tools, detailing their parameters and usage specifications. When tools like `fold_fragment` or `summarize_fragment` modify context content, the original text is temporarily stored in memory to enable complete restoration via `restore_fragment`. This ensures no information is permanently lost during context management operations.

1321
1322
1323
1324
1325
1326
1327
1328
1329
1330
1331
1332
1333
1334
1335
1336
1337
1338
1339
1340
1341
1342
1343
1344
1345
1346
1347
1348
1349

```

1350
1351
1352
1353
1354
1355
1356
1357
1358
1359 {
1360     "type": "function",
1361     "function": {
1362         "name": "fragment_context",
1363         "description": "Fragment conversation content between specified
1364             markers into manageable pieces. Useful for breaking down long
1365             text sections for detailed analysis.",
1366         "parameters": {
1367             "type": "object",
1368             "properties": {
1369                 "start_marker": {
1370                     "type": "string",
1371                     "description": "Start marker text to identify the beginning of
1372                         content to fragment"
1373                 },
1374                 "end_marker": {
1375                     "type": "string",
1376                     "description": "End marker text to identify the end of content
1377                         to fragment"
1378                 },
1379                 "num_fragments": {
1380                     "type": "integer",
1381                     "default": 5,
1382                     "minimum": 1,
1383                     "maximum": 20,
1384                     "description": "Number of fragments to create (default: 5)"
1385                 },
1386                 "role": {
1387                     "type": "string",
1388                     "enum": ["user", "assistant", "all"],
1389                     "default": "user",
1390                     "description": "Which role's messages to search in (default:
1391                         user)"
1392                 }
1393             }
1394         },
1395         "required": ["start_marker", "end_marker"],
1396         "additionalProperties": false
1397     }
1398 }
1399
1400
1401
1402
1403

```

Figure 14: JSON schema for `fragment_context` tool: Fragments conversation content between markers.

```

1404
1405
1406
1407
1408 {
1409     "type": "function",
1410     "function": {
1411         "name": "fold_fragment",
1412         "description": "Fold (hide) a conversation fragment to reduce visible
1413             context length. The content is preserved and can be expanded
1414             later.",
1415         "parameters": {
1416             "type": "object",
1417             "properties": {
1418                 "fragment_id": {
1419                     "type": "string",
1420                     "description": "ID of the fragment to fold (e.g., 'f1a2b3')"
1421                 }
1422                 },
1423             }
1424         }
1425
1426
1427     Figure 15: JSON schema for fold_fragment tool: Hides fragments to reduce context.
1428
1429
1430
1431
1432
1433
1434
1435
1436 }
1437     "type": "function",
1438     "function": {
1439         "name": "restore_fragment",
1440         "description": "Restore a fragment to its original content from ACM
1441             storage. Works for both summarized and folded fragments.",
1442         "parameters": {
1443             "type": "object",
1444             "properties": {
1445                 "fragment_id": {
1446                     "type": "string",
1447                     "description": "ID of the fragment to restore (e.g., 'f1a2b3')"
1448                 }
1449                 },
1450             }
1451         }
1452
1453
1454     Figure 16: JSON schema for restore_fragment tool: Restores modified fragments.
1455
1456
1457

```

```

1458
1459
1460
1461
1462
1463
1464
1465
1466
1467
1468
1469
1470
1471
1472
1473 {
1474     "type": "function",
1475     "function": {
1476         "name": "summarize_fragment",
1477         "description": "Summarize a conversation fragment using LLM to
1478             compress content while preserving key information. Supports focus
1479             -oriented summarization.",
1480         "parameters": {
1481             "type": "object",
1482             "properties": {
1483                 "fragment_id": {
1484                     "type": "string",
1485                     "description": "ID of the fragment to summarize (e.g., 'f1a2b3
1486                         ')"
1487                 },
1488                 "focus": {
1489                     "type": "string",
1490                     "description": "Focus area for the summary (e.g., 'technical
1491                         details', 'key decisions', 'action items', 'main points', '
1492                         problems', 'solutions')"
1493                 }
1494             },
1495             "required": ["fragment_id", "focus"],
1496             "additionalProperties": false
1497         }
1498     }
1499 }
1500
1501
1502
1503
1504
1505
1506
1507
1508
1509
1510
1511

```

Figure 17: JSON schema for summarize_fragment tool: Compresses fragments with LLM.

```

1512
1513
1514
1515
1516
1517
1518
1519
1520
1521
1522 {
1523     "type": "function",
1524     "function": {
1525         "name": "search_context",
1526         "description": "Search tool for finding exact text matches in
1527             conversation history.",
1528         "parameters": {
1529             "type": "object",
1530             "properties": {
1531                 "query": {
1532                     "type": "string",
1533                     "description": "Exact text to search for in conversation
1534                         history"
1535                 },
1536                 "role": {
1537                     "type": "string",
1538                     "enum": ["user", "assistant", "all"],
1539                     "default": "user",
1540                     "description": "Filter by message role (default: user)"
1541                 },
1542                 "max_results": {
1543                     "type": "integer",
1544                     "default": 10,
1545                     "minimum": 1,
1546                     "maximum": 50,
1547                     "description": "Maximum number of results to return"
1548                 },
1549                 "context_size": {
1550                     "type": "integer",
1551                     "default": 200,
1552                     "minimum": 50,
1553                     "maximum": 1000,
1554                     "description": "Context characters before/after match"
1555                 },
1556             },
1557             "required": ["query"],
1558             "additionalProperties": false
1559         }
1560     }
1561 }
1562
1563
1564
1565

```

Figure 18: JSON schema for `search_context` tool: Exact text search in conversation.

```

1566
1567
1568
1569
1570
1571
1572
1573
1574
1575
1576
1577
1578
1579
1580
1581 {
1582     "type": "function",
1583     "function": {
1584         "name": "get_search_detail",
1585         "description": "Get detailed context for a search result by its ID.  
Retrieves extended context around the search match position.",
1586         "parameters": {
1587             "type": "object",
1588             "properties": {
1589                 "search_id": {
1590                     "type": "string",
1591                     "description": "Search result ID from search_context (e.g., 's1a2b3')"
1592                 },
1593                 "extended_context": {
1594                     "type": "integer",
1595                     "default": 500,
1596                     "minimum": 100,
1597                     "maximum": 2000,
1598                     "description": "Number of characters to show before and after  
the match (default: 500)"
1599                 },
1600                 "required": ["search_id"],
1601                 "additionalProperties": false
1602             }
1603         }
1604
1605
1606     Figure 19: JSON schema for get_search_detail tool: Retrieves extended context.
1607
1608
1609
1610
1611
1612
1613
1614
1615
1616
1617
1618
1619

```